NASA MEMO 3-3-59H

NASA

MEMORANDUM

A SUMMARY OF FLIGHT-DETERMINED TRANSONIC LIFT AND DRAG CHARACTERISTICS OF SEVERAL RESEARCH AIRPLANE CONFIGURATIONS

By Donald R. Bellman

High-Speed Flight Station
Edwards, Calif.

NATIONAL AERONAUTICS AND SPACE ADMINISTRATION

WASHINGTON

April 1959

Declassified May 29, 1961

A

NATIONAL AERONAUTICS AND SPACE ADMINISTRATION

MEMORANDUM 3-3-59H

H
1
1
3

A SUMMARY OF FLIGHT-DETERMINED TRANSONIC LIFT AND DRAG CHARACTERISTICS OF SEVERAL RESEARCH AIRPLANE CONFIGURATIONS

By Donald R. Bellman

SUMMARY

Flight-determined lift and drag data from transonic flights of seven research airplane configurations of widely varying characteristics are presented and compared with wind-tunnel and rocket-model data. The airplanes are the X-5 (59° wing sweep), XF-92A, YF-102 with cambered wing, YF-102 with symmetrical wing, D-558-II, X-3, and X-1E. The effects of some of the basic configuration differences on the lift and drag characteristics are demonstrated. As indicated by transonic similarity laws, most of the configurations demonstrate a relationship between the transonic increase in zero-lift drag and the maximum cross-sectional area. No such relationship was found between the drag-rise Mach number and its normally related parameters. A comparison of flight and wind-tunnel data shows a generally reasonable agreement, but Reynolds number differences can cause considerable variations in the drag levels of the flight and wind-tunnel tests. Maximum lift-drag ratios vary widely in the subsonic region as would be expected from differences in aspect ratio and wing thickness ratio; however, the variations diminish as the Mach number is increased through the transonic region. The attainment of maximum lift-drag ratio in level flight by several of the airplanes was limited by engine performance, stability characteristics, and buffet boundaries.

INTRODUCTION

In most of the tests performed with research airplanes at the NASA High-Speed Flight Station, Edwards, Calif., lift and drag characteristics were obtained and subsequently reported in numerous papers. This paper consolidates the previously reported data, presents data obtained since

the preparation of the original papers, and makes additional comparisons with model data. It should be noted that the airplanes considered in this paper differ from one another in many aspects and were designed at different times and for different purposes. Consequently, the data cannot be used as a means of comparing single characteristics such as plan form, wing sweep, or aspect ratio. The comparisons presented are intended to show the general range of aerodynamic characteristics covered by these configurations.

Transonic lift and drag data for the following airplanes are presented: X-5 (59° wing sweep), XF-92A, YF-102 with cambered wing, YF-102 with symmetrical wing, D-558-II, X-3, and X-1E. The data for these airplanes were originally published in references 1 to 5. Additional unpublished data have been used as noted.

SYMBOLS

A	cross-sectional area, sq ft
AR	aspect ratio
C_D	drag coefficient, D/qS
$C_{D_{DR}}$	drag coefficient at the drag-rise Mach number
C_{D_0}	drag coefficient at zero lift
C_L	lift coefficient, L/qS
C_{L_α}	lift-curve slope, deg^{-1}
c	chord
D	drag force, lb
$dC_D/dC_L{}^2$	drag-due-to-lift factor
ΔC_D	transonic drag-coefficient increment, $\left(C_{D_{max}}\right)_{M>1} - C_{D_{DR}}$
g	gravitational acceleration, ft/sec^2
h_p	pressure altitude, ft

	L	lift force, lb
	l	fuselage length, ft
H	M	Mach number
l		
l	q	dynamic pressure, lb/sq ft
3		
	S	wing area, sq ft
	t/c	maximum wing thickness ratio
	x	distance along fuselage from nose, ft
	α	angle of attack, deg

Subscript:

max	maximum

AIRPLANES AND TESTS

The seven research airplane configurations for which data are presented are single place and are capable of transonic or supersonic speeds. Figure 1 shows a two-view sketch of each airplane drawn to approximately the same scale. Figure 2 presents photographs of each airplane. Pertinent dimensions and details of the airplanes are listed in table I. The weights and wing loadings for normal flight were determined by assuming 30-percent fuel remaining.

Although all the airplanes were designed before the area rule was recognized as an important design tool, area differences in these airplanes demonstrate some of the area-rule principles; the cross-sectional-area distributions are shown, therefore, in figure 3. The area distributions are presented on a nondimensional basis by dividing the cross-sectional areas by the wing areas, instead of dividing by the more commonly used fuselage length squared. The use of wing area for nondimensionalizing makes the parameter more nearly comparable to airplane drag, inasmuch as drag coefficients are also based on unit wing area. For the airplanes with internal ducts, approximately 85 percent of the minimum duct area has been removed from the fuselage cross-sectional area and is shown as a dotted line at the lower part of each diagram.

Additional features of the airplanes and the test conditions under which the data were obtained are described in the following subsections.

X-5 Airplane

The Bell X-5 research airplane is constructed so that the wing-sweep angle can be varied in flight from 20° to 59°. Of the configurations tested only the 59° configuration has sonic speed capabilities; therefore, only this configuration is presented. The airplane is powered by a J35-A-17 turbojet engine and is capable of a Mach number of 0.94 in level flight or about 1.07 in a dive. Lift and drag data for this airplane were presented originally in reference 1; however, the data used herein are from flights subsequent to those of reference 1. In the flights of reference 1 the thrust was estimated from altitude-wind-tunnel data of the engine, whereas in the later flights the thrust was measured with duct and tailpipe probes. Significant differences in the data were observed only at the lower Mach numbers. The bulk of the data was obtained at altitudes between 38,000 feet and 43,000 feet; a small amount of the data was obtained at altitudes down to 25,000 feet. The Reynolds numbers based on the mean aerodynamic chord varied from 10×10^6 to 26×10^6.

XF-92A Airplane

The Convair XF-92A airplane has a 60° delta wing and no horizontal tail. It is powered by a J33-A-29 turbojet engine-afterburner combination and has approximately the same speed capabilities as the X-5 airplane. Some lift and drag data for the XF-92A airplane are presented in reference 2. The data used in this paper were obtained primarily from later flights in which much greater lift ranges were covered. The general level of drag of the later flights is slightly, but measurably, higher than the previously reported flights. It is believed that this higher level of drag is the result of certain fuselage modifications including the addition of engine-cooling airscoops. The Reynolds numbers based on the mean aerodynamic chord varied from 40×10^6 to 55×10^6.

YF-102, Cambered Wing, and YF-102, Symmetrical Wing, Airplanes

The Convair YF-102 airplane, similar to the XF-92A airplane, has a 60° delta wing and no horizontal tail. It differs from the XF-92A airplane in three significant ways: it has a 4-percent-thick wing rather than a 6.5-percent-thick wing, it has side inlets instead of a nose inlet, and the trailing edge of the wing is swept forward 5°. The airplane was originally equipped with a symmetrical sectional wing having

a single pair of fences. After tests were completed with this configuration, a cambered leading edge was installed on the wing. Concurrently, a second pair of fences was added inboard of the other fences, and the wing tips outboard of the elevon were reflexed 10° up at the trailing edge. The modifications caused considerable variation in the lift and drag characteristics; therefore, data from reference 3, for both configurations are presented. The Reynolds numbers based on the mean aerodynamic chord varied from 23×10^6 to 77×10^6.

D-558-II Airplane

Two versions of the Douglas D-558-II research airplane were investigated; one powered by both a J34-WE-40 turbojet engine and an LR8-RM-6 rocket engine; the other powered only by an LR8-RM-6 rocket engine. The wing and tail surfaces on the two versions were identical and, except for ducts, the fuselages were essentially the same. Since no significant difference in the drag data for the two versions was observed, data from both configurations are included. Some of the data from the all-rocket airplane were obtained from reference 4; the remainder is unpublished data from both airplanes. The all-rocket airplane is capable of Mach numbers up to 2.0 and altitudes in excess of 80,000 feet. The turbojet and rocket version is limited to speeds only slightly greater than sonic speed and altitudes of about 40,000 feet. Data at Mach numbers of 0.90 and 0.96 were obtained with the rocket- and turbojet-powered airplane with Reynolds numbers based on the mean aerodynamic chord varying from 15×10^6 to 19×10^6. The remainder of the data was obtained with the all-rocket airplane at Reynolds numbers varying from 12×10^6 to 17×10^6.

X-3 Airplane

The Douglas X-3 research airplane has a straight wing of low aspect ratio with a sharp leading edge. The wing loading can be as high as 132 pounds per square foot on take-off. The airplane is powered by two J34-WE-17 turbojet-afterburner combinations and is capable of a Mach number of about 1.2 in a dive. The data presented were taken from reference 5. Reynolds numbers based on the mean aerodynamic chord varied from 13×10^6 to 37×10^6.

X-1E Airplane

The X-1E airplane is an NASA revision of the Bell X-1, no. 2, airplane, one of the original pair of X-1 airplanes. The early airplanes

had heavy-walled propellant tanks, and high-pressure gas was used to transfer the propellants to the engine. In the revisions that created the X-1E the propellant tanks were replaced with lightweight versions, and the propellants fed to the engine by means of a hydrogen-peroxide-driven pump. The change greatly increased the fuel capacity. In addition, a new wing was installed, reducing the thickness ratio from 10 percent to about 4 percent and the aspect ratio from 6 to 4. The original 8-percent-thick horizontal tail was retained. The fuselage nose was altered to incorporate an ejection seat and a raised top-opening canopy to provide a means of escape and better vision.

The X-1E version not only had increased fuel capacity, but also had greatly decreased drag in the transonic and supersonic regions as a result of the decrease in wing thickness. Consequently, the maximum Mach number of the airplane was increased from about 1.5 to greater than 2.2. The drag of the early versions of the airplane was presented in references 6 and 7. Reynolds numbers based on mean aerodynamic chord for the X-1E flights varied from 5×10^6 to 15×10^6.

ACCURACY

Lift

The accuracy of the flight lift coefficients is dependent primarily on the accuracy of the normal-acceleration measurement, which was 0.05g for each of the airplanes. The error in lift coefficient would then be a function of wing loading and dynamic pressure. The accuracy increases as the dynamic pressure becomes higher and the wing loading becomes lower. At an altitude of about 35,000 feet and at a Mach number of 0.90, the error in lift coefficient would be 0.005 for the XF-92A airplane and 0.019 for the X-3 airplane. The accuracy of lift coefficient of model data used later in this paper for comparative purposes varies from 0.003 for the Ames 6- by 6-foot supersonic tunnel and 0.001 for the Langley 8-foot transonic tunnel to 0.05 for rocket models at low speeds.

Drag

The accuracy of flight drag coefficients is almost equally dependent on three, and sometimes four, quantities: airplane weight, angle of attack, longitudinal acceleration, and thrust. A detailed discussion of errors in these quantities is presented in reference 8. Some of the special conditions arising in the tests covered by this paper are given in the following sections.

Airplane weight.- Measurement of airplane weight is of particular significance only for rocket airplanes, since their enormous fuel consumption makes the weight accurate to only 1 percent as compared to turbojet-powered airplanes for which weight generally is known to less than one-half of 1 percent.

Angle of attack.- Error in angle of attack can be appreciable, but it affects drag coefficients only in proportion to the lift and, therefore, has no effect on the zero-lift drag. The principal sources of error in angle-of-attack measurements are instrument error, airplane pitching effects, boom bending due to both airloads and acceleration loads, vane floating arising from slight asymmetry, and upwash due to the wing, fuselage, and airspeed boom.

Most of the airplanes had turnmeters, making it possible to correct for pitching velocities. Such corrections were made where necessary for a small part of the data from the XF-92A and X-3 airplanes and were made routinely for the YF-102 and X-1E airplanes.

Boom bending due to normal acceleration was considered on all airplanes except the X-1E which had a short stiff boom. The correction varied from 0.09° per g for the relatively stiff boom of the D-558-II airplane to 0.16° per g for the XF-92A airplane.

Upwash affects the angle-of-attack measurements to only a minor extent on most of the airplanes, therefore upwash corrections were not made. Corrections were considered, however, for the X-1E airplane where the vane blade was 29 inches ahead of the fuselage and 202.5 inches ahead of the quarter chord of the wing. In comparison, the angle-of-attack-vane blade of the X-3 airplane was more than 500 inches ahead of the wing quarter chord.

Longitudinal acceleration.- Longitudinal accelerations were originally measured with the standard NASA three-component accelerometer with an accuracy of about 0.02g. The instruments were air-damped, and the accuracy deteriorated somewhat at the higher altitudes. Such instruments were used on the XF-92A (tests reported in ref. 2) and X-3 airplanes. An NASA magnetically damped instrument having an accuracy of 0.01g was used on the X-1E, XF-92A (tests reported herein), D-558-II, X-5, and YF-102 airplanes. The accelerometer must be alined with the axis of the airplane within 0.1° to prevent a significant carryover from the normal acceleration. It is doubtful that such care in mounting was given the earlier installations.

Thrust.- Thrust must be measured within 100 pounds to prevent excessive error in drag. This accuracy is easily attained on the rocket engines of the D-558-II and the X-1E airplanes, but a rather elaborate system of rakes is required to achieve the same accuracy on jet engines.

The estimated thrust accuracy of the XF-92A airplane was 200 pounds, primarily because of difficulties in measuring the air flow in a centrifugal-type jet engine.

Mach Number

The airplanes had well-calibrated airspeed heads which, for the Mach number range covered by this paper, resulted in Mach numbers accurate to within 0.01.

RESULTS AND DISCUSSION

Lift

The variations of lift coefficient with angle of attack for the seven airplane configurations are presented in figure 4 for representative Mach numbers in the transonic region. Also shown in figure 4 are comparable wind-tunnel data taken from references 9 to 14 and from unpublished sources. With the exception of the XF-92A airplane, the flight data are for trim conditions, whereas the wind-tunnel data except for the X-5 and YF-102 airplanes are for zero elevator and stabilizer deflections. In general, the stabilizer and elevator have only a minor effect on the lift curves, therefore such comparisons are valid. For the tailless XF-92A and YF-102 airplanes, however, the elevon position has a large effect on the lift, as indicated by reference 2 which shows that trim elevon deflection causes a 20- to 25-percent decrease in lift-curve slope over the Mach number range from 0.6 to 0.95. Since tunnel data for the XF-92A airplane were available only for zero elevon deflection, the flight data were corrected to zero elevon deflection using wind-tunnel data from reference 10 as a basis. Since no model tested in reference 10 was an exact model of the XF-92A, the flight data are compared with the open-nose-entry model which had the proper wing and vertical tail but a fuselage 34 percent larger in diameter, scalewise, than the actual airplane. The wind-tunnel data for both YF-102 airplane configurations are unpublished data from the NASA-Langley 8-foot transonic wind tunnel. These data were available for various elevon positions and were selected to correspond to flight trim conditions. The wind-tunnel data for the X-5 and X-1E airplanes were also selected to correspond to flight trim conditions. For the X-3 airplane both the tunnel data and flight data were limited so that comparable lift and drag curves were available only at a Mach number of 0.90. Therefore, a comparison was also made with rocket-model tests at four Mach numbers in the transonic region.

In general, the flight lift data compare well with the tunnel data, usually falling within the stated accuracies of the measurements. The slopes of the lift curves for the seven airplane configurations at lift coefficients of approximately 0.3 are shown in figure 5. All data are for flight trim conditions. The exact shape and level of the curve depend on numerous factors such as aspect ratio, wing thickness, wing sweep, and airfoil section. None of these configurations demonstrates the transonic dips in the variation of the lift-curve slope with Mach number which was characteristic of the original X-1 airplanes (see refs. 6 and 7). Reference 15 demonstrates that the occurrence of such dips, or "buckets," is a function of wing-thickness ratio and aspect ratio. Figure 4 of reference 15 shows approximate boundaries, indicating that the original X-1 airplanes should experience these dips, that the X-1E, X-3, XF-92A, YF-102, and X-5 airplanes should not, and that the D-558-II airplane is on the borderline. The flight tests substantiate these predictions. The X-5, XF-92A, and YF-102 airplanes have lift-curve slopes that are distinctly lower and vary less with Mach number than those of the other three airplanes. This condition probably occurs because the X-5, XF-92A, and YF-102 airplanes have not only the lowest aspect ratios, but also the greatest amount of wing sweep.

H
1
1
3

Drag

The variation of drag coefficient with lift coefficient at various constant Mach numbers is shown in figure 6 for the seven airplane configurations, together with a comparison with wind-tunnel data. No comparison is made for the XF-92A, because of the magnitude of the corrections for variations in elevon positions and because of the lack of suitable data on which to base such a correction. In figure 6 all flight data are for flight trim conditions; wind-tunnel data for the X-5, YF-102, and X-1E airplanes are also for flight trim conditions. The wind-tunnel data for the D-558-II and X-3 airplanes are for horizontal stabilizer and elevator settings of zero. The X-3 rocket-model data were taken at fixed horizontal stabilizer deflections of -1.25° for Mach numbers of 0.89 and 1.04 and -2.80° for Mach numbers of 0.97 and 1.14. On the whole, fair agreement is shown between the flight and model data. It should be noted that poorer agreement would be expected for the Mach numbers in the drag-rise region where slight changes in Mach number can result in appreciable differences in drag coefficient. Presumably, this condition is applicable to the X-5 airplane where flight data at a Mach number of 0.97 are compared with wind-tunnel data at a Mach number of 0.96.

A further comparison of the flight and wind-tunnel drag data is made in figure 7 in which the variation of drag coefficient with Mach number for constant low values of lift coefficient is shown. In the drag-rise Mach number region considerable discrepancy exists between

the flight and model data for some of the configurations. It is believed that these discrepancies are not necessarily a reflection on the accuracy of the data, but in many cases may be attributed to factors such as model differences, internal-flow differences, base pressure effects, and Reynolds number effects. For example, both the X-5 and X-3 airplane models had enlarged fuselage bases to allow for the sting mounting. Reference 3 shows how Reynolds number variation between flight and model tests of the YF-102 airplane could cause differences of 0.003 in drag coefficient which amount to 20 or 30 percent of the low-lift subsonic drag coefficients. The only model data available for comparison with the X-1E data were from a 1/62-scale model tested at high supersonic Mach numbers. Reynolds numbers for the model tests were less than one-tenth those for the full-scale flight tests. The effect of such Reynolds number differences was calculated from the basic data of reference 16 which were converted to high Mach numbers by using data of reference 17. The calculations showed that the model tests would have skin-friction drag coefficients at least 0.0090 higher than the flight tests, which is about the amount of the differences in the data shown in figures 6(g) and 7(g). The calculations assumed fully turbulent flow for both the flight and the model tests; the assumption is justified for the model despite the low Reynolds numbers because transition strips were used.

Because of the widely varying characteristics of the seven airplane configurations, it is interesting to compare their transonic drag characteristics in the light of various parameters. In figure 8 the airplanes are compared on the basis of increase in drag coefficient above the drag-rise Mach number which is arbitrarily defined as the Mach number where the rate of change of drag coefficient with Mach number $\left(dC_D/dM\right)$ first becomes 0.1. Transonic similarity rules show that the transonic drag-coefficient increment for a wing alone will vary with $(t/c)^{5/3}$ (ref. 18). The similarity between the quantities t/c and A/S would indicate a similar relationship between the transonic drag-coefficient increment and $(A/S)^{5/3}$. In figure 9 the transonic drag-coefficient increment is plotted against the quantity $(A/S)^{5/3}$, and it can be seen that, with the exception of the X-3 airplane, the data presented closely approximate a straight line.

The drag-rise Mach number is a measure of the Mach number at which appreciable portions of the air flow adjacent to the airplane reach sonic velocity. Reference 19 indicates that for wings, the drag-rise Mach number is primarily a function of wing thickness ratio and wing sweep angle. For complete airplanes, it undoubtedly is also a function of cross-sectional-area distribution. Comparing the subject airplane configuration on the basis of these three parameters shows poor

correlation, and it is probable that the airplanes are sufficiently different that no one factor is dominant in determining the drag-rise Mach number in all cases.

The effect of lift on drag is shown in figure 10 where the square of the lift coefficient is plotted against the drag coefficient for the subsonic, transonic, and supersonic speed ranges. Drag data at a constant Mach number when plotted in this manner approximate a straight line and the slope termed drag-due-to-lift factor can be used as a measure of the drag at lifting conditions. For some of the airplanes the approximation of a straight line is relatively poor in the transonic region. In the supersonic region the approximation is good for most of the airplanes; only the D-558-II airplane shows appreciable curvature.

The drag-due-to-lift factors were determined for the airplanes over the Mach number range at a lift coefficient of about 0.3. The results are presented in figure 11. It should be noted that the drag-due-to-lift factors are the actual slopes of the curves of figure 10 at a lift coefficient of 0.3; hence, the drag equation $C_D = C_{D_0} + \frac{dC_D}{dC_L^2} C_L^2$ will apply only in those cases where C_D plotted against C_L^2 is a straight line between a lift coefficient of 0 and 0.3. Aerodynamic theory shows that for subsonic conditions the drag-due-to-lift factor will equal $1/C_{L_\alpha}$ if there is no leading-edge suction and will approximate $1/\pi AR$ if the leading-edge suction is fully developed. A comparison of the subsonic data of figure 11 with comparable data of figure 5 shows that none of the seven airplane configurations closely approaches fully developed leading-edge-suction conditions. As would be expected, the airplane with the greatest wing-thickness ratio, the D-558-II airplane, shows the greatest amount of leading-edge suction. Reference 20 indicates that low-aspect-ratio thin wings lose a considerable portion of their leading-edge suction. The X-3 airplane, for example, would not have any significant amount of leading-edge suction because of the sharp leading edge of its wing. The drag-due-to-lift factors of the XF-92A airplane are increased further over what would be expected of this wing type because trim data are used which include a simultaneous increase in elevon deflection with an increase in lift. Since an increase in elevon deflection causes a loss in lift, a considerably greater angle of attack is required to create a given lift under trim conditions than with zero elevon deflection. Figure 12 shows a comparison of drag-due-to-lift factors for the X-3 and D-558-II airplanes with the $1/\pi AR$ and $1/C_{L_\alpha}$ values for these airplanes. The D-558-II curve deviates considerably from the zero suction curve $1/C_{L_\alpha}$ toward the full suction curve $1/\pi AR$ at the lower Mach numbers, indicating a considerable amount of leading-edge suction at these

Mach numbers. The drag-due-to-lift factor for the X-3 airplane is even higher than would be indicated by the expected complete lack of leading-edge suction. This condition is possibly the result of fuselage effects such as base drag which can vary considerably with lift. The X-3 airplane has a large amount of fuselage area in comparison to its wing area.

Lift-Drag Ratio

The best measure of the overall efficiency of an airplane at any given Mach number is the lift-drag ratio, which for level flight is the reciprocal of the drag force per unit airplane weight. The maximum lift-drag ratios of the seven airplane configurations are plotted against Mach number in figure 13. In the subsonic region, as might be expected from the wide variation in aspect ratios of the airplanes, there is a wide variation in maximum lift-drag ratio which greatly diminishes as the Mach number is increased through the transonic region.

In discussing maximum lift-drag ratios, the ability of the airplane to fly at the required conditions must be considered, since buffeting, control, and engine-operation limitations may prevent such operation. Figure 14 presents the lift coefficients at which the maximum lift-drag ratios of figure 13 are obtained. Figure 15 shows the altitude required for the airplanes to fly in level flight at these specified lift coefficients. The data of figure 15 were calculated by using the normal flight wing loadings given in table I. The X-5, X-3, and XF-92A airplanes are limited by their engine capabilities to altitudes below 45,000 feet; the YF-102 airplane cannot exceed 55,000 feet. Therefore, it is evident that these airplanes will be able to attain their maximum lift-drag ratios in level flight only in the subsonic and low transonic region. Also, the D-558-II airplane is restricted by the instability and buffet boundaries. Reference 21 shows that this airplane, when at a lift coefficient for maximum lift-drag ratio, will encounter heavy buffeting at a Mach number of 0.90 and longitudinal instability at a Mach number of 0.92.

CONCLUDING REMARKS

Flight data from seven widely varying research airplane configurations are compiled and compared with applicable wind-tunnel and rocket-model data. A comparison of the flight and wind-tunnel data shows that, generally, reasonable agreement exists, but Reynolds number differences can cause considerable variations in the results.

In accordance with theoretical predictions, none of the seven configurations shows the transonic dips in the variation of lift-curve slope with Mach number which are characteristic of wings of higher

aspect and thickness ratios, such as the original X-1 airplanes. As might be expected from transonic similarity laws, all the configurations except the X-3 indicate a linear relationship between the transonic increase in zero-lift drag and the five-thirds power of the maximum ratio of cross-sectional area to wing area. The drag-rise Mach number does not appear to be dependent on any one factor such as wing-thickness ratio, aspect ratio, wing-sweep angle, and maximum cross-sectional area.

Maximum lift-drag ratios vary widely in the subsonic region as would be expected from the differences in aspect ratio and wing-thickness ratio; however, the variations diminish as the Mach number is increased through the transonic region. The attainment of maximum lift-drag ratio in level flight by several of the airplanes is limited by altitude, stability, and buffet boundaries.

High-Speed Flight Station,
National Aeronautics and Space Administration,
Edwards, Calif., December 10, 1958.

REFERENCES

1. Bellman, Donald R.: Lift and Drag Characteristics of the Bell X-5 Research Airplane at 59° Sweepback for Mach Numbers From 0.60 to 1.03. NACA RM L53A09c, 1953.

2. Bellman, Donald R., and Sisk, Thomas R.: Preliminary Drag Measurements of the Consolidated Vultee XF-92A Delta-Wing Airplane in Flight Tests to a Mach Number of 1.01. NACA RM L53J23, 1954.

3. Saltzman, Edwin J., Bellman, Donald R., and Musialowski, Norman T.: Flight-Determined Transonic Lift and Drag Characteristics of the YF-102 Airplane With Two Wing Configurations. NACA RM H56E08, 1956.

4. Nugent, Jack: Lift and Drag Characteristics of the Douglas D-558-II Research Airplane Obtained in Exploratory Flights to a Mach Number of 2.0. NACA RM L54F03, 1954.

5. Bellman, Donald R., and Murphy, Edward D.: Lift and Drag Characteristics of the Douglas X-3 Research Airplane Obtained During Demonstration Flights to a Mach Number of 1.20. NACA RM H54I17, 1954.

6. Carman, L. Robert, and Carden, John R.: Lift and Drag Coefficients for the Bell X-1 Airplane (8-Percent-Thick Wing) in Power-Off Transonic Flight. NACA RM L51E08, 1951.

7. Saltzman, Edwin J.: Flight Measurements of Lift and Drag for the Bell X-1 Research Airplane Having a 10-Percent-Thick Wing. NACA RM L53F08, 1953.

8. Beeler, De E., Bellman, Donald R., and Saltzman, Edwin J.: Flight Techniques for Determining Airplane Drag at High Mach Numbers. NACA TN 3821, 1956.

9. Bielat, Ralph P., and Campbell, George S.: A Transonic Wind-Tunnel Investigation of the Longitudinal Stability and Control Characteristics of a 0.09-Scale Model of the Bell X-5 Research Airplane and Comparison With Flight. NACA RM L53H18, 1953.

10. Lawrence, Leslie F., and Summers, James L.: Wind-Tunnel Investigation of a Tailless Triangular-Wing Fighter Aircraft at Mach Numbers From 0.5 to 1.5. NACA RM A9B16, 1949.

11. Kelly, Thomas C.: Transonic Wind-Tunnel Investigation of the Effects of External Stores and Store Position on the Aerodynamic Characteristics of a 1/16-Scale Model of the Douglas D-558-II Research Airplane. NACA RM L55I07, 1955.

12. Olson, Robert N., and Chubb, Robert S.: Wind-Tunnel Tests of a 1/12-Scale Model of the X-3 Airplane at Subsonic and Supersonic Speeds. NACA RM A51F12, 1951.

13. Peck, Robert F., and Hollinger, James A.: A Rocket-Model Investigation of the Longitudinal Stability, Lift, and Drag Characteristics of the Douglas X-3 Configuration With Horizontal Tail of Aspect Ratio 4.33. NACA RM L53F19a, 1953.

14. Henderson, Arthur, Jr.: Wind-Tunnel Investigation of the Static Longitudinal and Lateral Stability of a 1/62-Scale Model of the X-1E at Supersonic Speeds. NACA RM L56C23b, 1956.

15. Donlan, Charles J., and Weil, Joseph: Characteristics of Swept Wings at High Speeds. NACA RM L52A15, 1952.

16. Van Driest, E. R.: Turbulent Boundary Layer in Compressible Fluids. Jour. Aero. Sci., vol. 18, no. 3, Mar. 1951, pp. 145-160, 216.

17. Rubesin, Morris W., Maydew, Randall C., and Varga, Steven A.: An Analytical and Experimental Investigation of the Skin Friction of the Turbulent Boundary Layer on a Flat Plate at Supersonic Speeds. NACA TN 2305, 1951.

18. Spreiter, John R.: Theoretical and Experimental Analysis of Transonic Flow Fields. NACA-University Conference on Aerodynamics, Construction, and Propulsion, Lewis Flight Propulsion Lab., Cleveland, Ohio, Oct. 20-22, 1954. vol. II.

19. Polhamus, Edward C.: Summary of Results Obtained by Transonic-Bump Method on Effects of Plan Form and Thickness on Lift and Drag Characteristics of Wings at Transonic Speeds. NACA RM L51H30, 1951.

20. Polhamus, Edward C.: Drag Due to Lift at Mach Numbers Up to 2.0. NACA RM L53I22b, 1953.

21. Fischel, Jack: Effect of Wing Slats and Inboard Wing Fences on the Longitudinal Stability Characteristics of the Douglas D-558-II Research Airplane in Accelerated Maneuvers at Subsonic and Transonic Speeds. NACA RM L53L16, 1954.

TABLE I

DIMENSIONS AND DETAILS OF THE SEVEN AIRPLANE CONFIGURATIONS

Characteristics	Airplanes						
	X-5	XF-92A	YF-102 Cambered wing	YF-102 Symmetrical wing	D-558-II	X-3	X-1E
Wing:							
Airfoil							
Root	NACA $64_{(10)}$A011	NACA $65_{(06)}$006.5	NACA 0004-65 mod.	NACA 0004-65 mod.	NACA 63-010	Modified hexagon	NACA 64A-004 mod.
Tip	NACA $64_{(08)}$A008.28	NACA $65_{(06)}$006.5	NACA 0004-65 mod.	NACA 0004-65 mod.	NACA 63_1-012	Modified hexagon	NACA 64A-004 mod.
Direction	Normal to 0.3802c	Streamwise	Streamwise	Streamwise	Normal to 0.30c	----------	Streamwise
Thickness (streamwise)							
Root, percent c	6.9	6.5	3.9	4.0	8.8	4.5	4.0
Tip, percent c	4.6	6.5	3.5	4.0	9.6	4.5	4.0
Sweep, deg	62.2 at L.E. 58.7 at 0.25c	60.0 at L.E. 52.4 at 0.25c	60.1 at L.E.	60.0 at L.E.	38.8 at L.E. 35.0 at 0.30c	23.2 at L.E. 0 at 0.75c	7.62 at L.E. 0 at 0.40c
Aspect ratio	2.16	2.31	2.08	2.20	3.57	3.09	3.99
Taper ratio	0.410	0	0.023	0	0.565	0.389	0.500
Incidence							
Root, deg	0	0	0	0	3.0	0	2.0
Tip, deg	0	0	0	0	3.0	0	2.0
Dihedral, deg	0	0	0	0	-3.0	0	0
Mean aerodynamic chord, ft	10.05	18.09	23.76	23.13	7.28	7.84	5.93
Area, sq ft	184.3	425.0	695.0	661.5	175.0	166.5	130.06
Span, ft	20.0	31.3	38.11	37.03	25.0	22.7	22.79
Wing loading, normal flight, lb/sq ft	46.0	30.4	32.4	33.6	64.8	108.4	80.5
Fuselage:							
Length, ft	31.7	42.8	52.4	52.4	42.0	63.5	31.0
Airplane weight, lb:							
Take-off	9,960	15,560	27,215	26,860	15,787	22,100	15,950
Empty	7,850	11,808	20,532	20,280	9,421	16,320	8,120
Normal flight	8,480	12,940	22,540	22,250	11,330	18,050	10,470

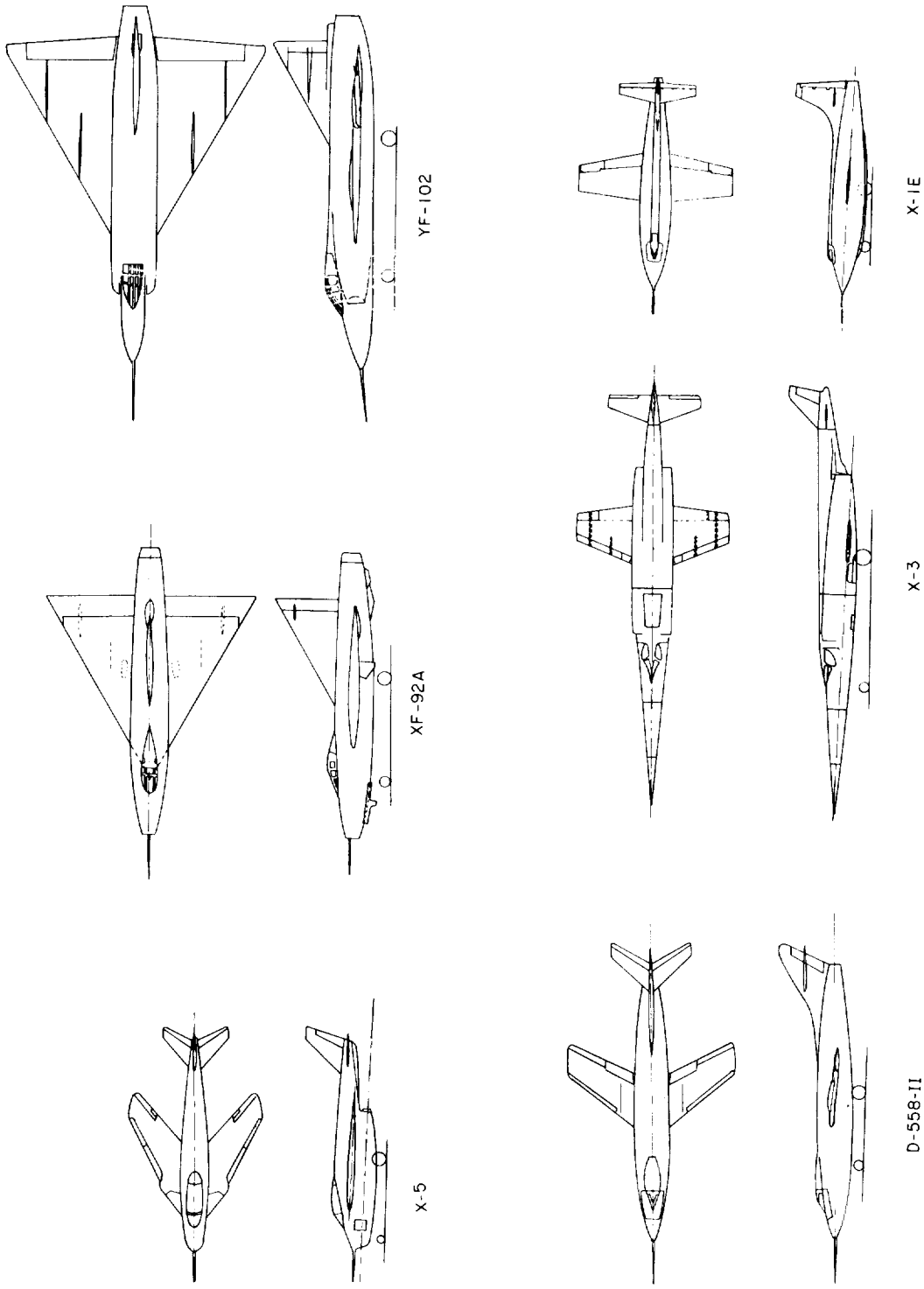

Figure 1.- Two-view sketches of the airplanes.

(a) X-5 airplane. E-813

Figure 2.- Photographs of the airplanes.

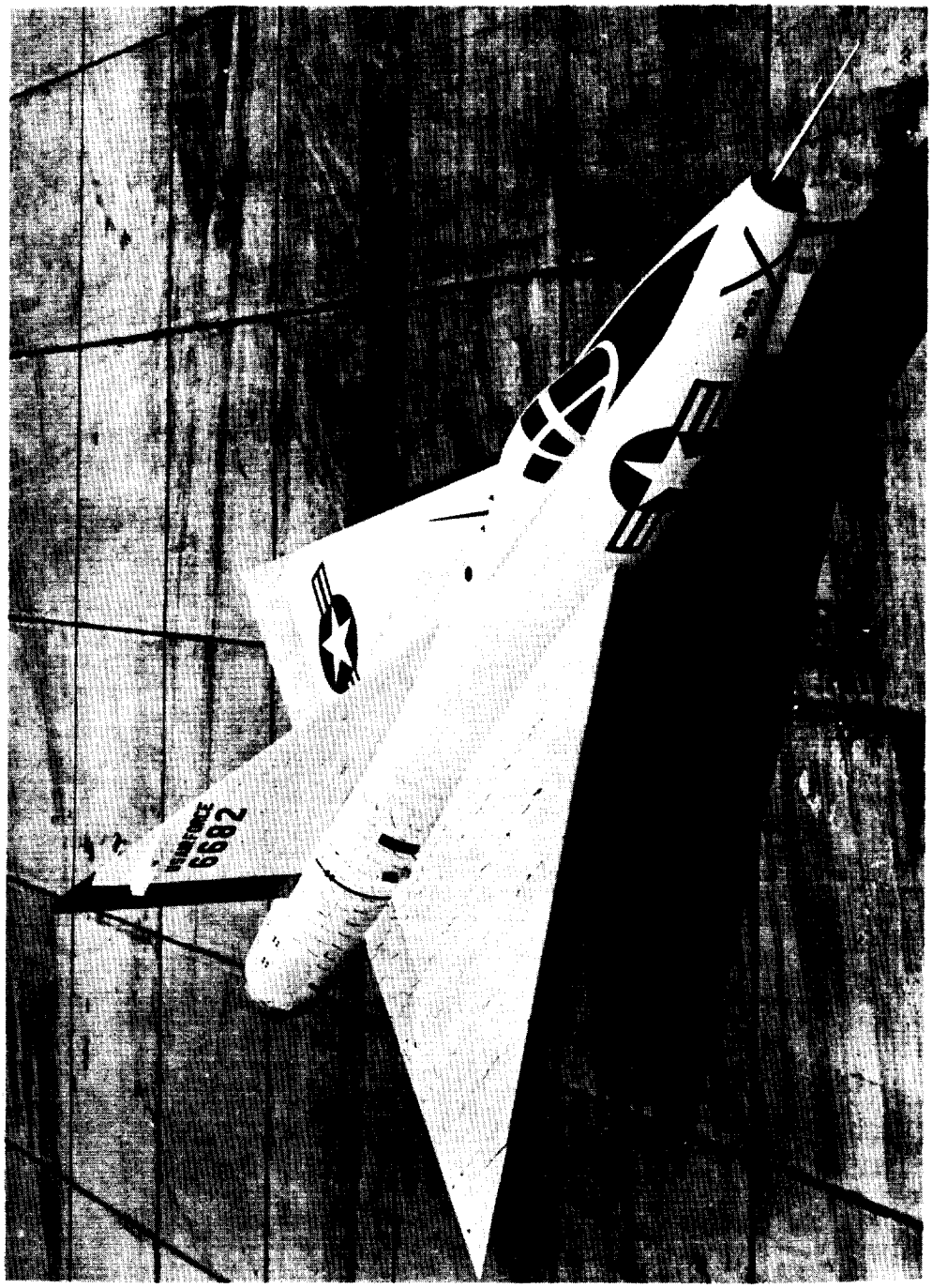

(b) XF-92A airplane. E-954

Figure 2.- Continued.

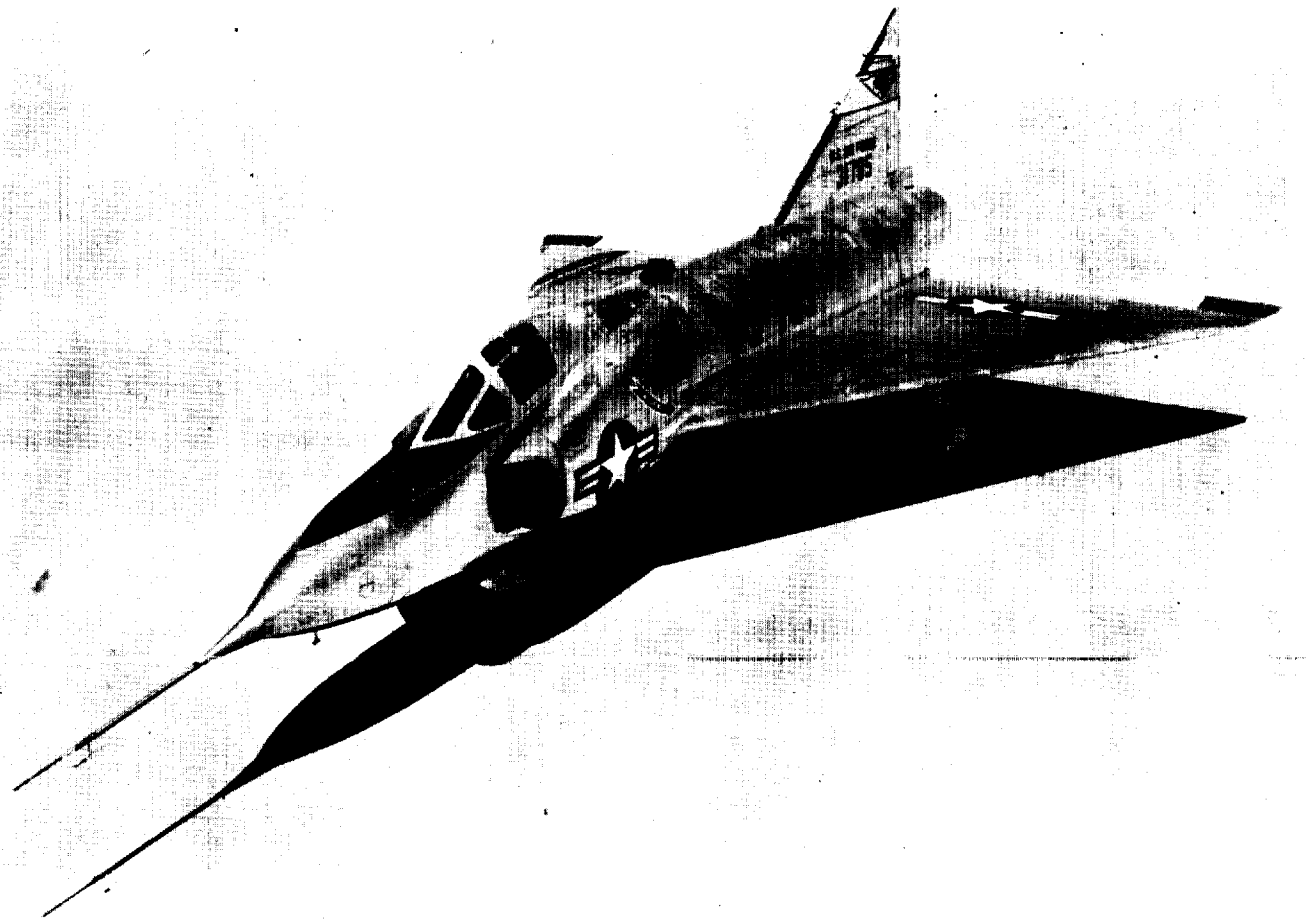

(c) YF-102 (cambered wing) airplane. E-1746

Figure 2.- Continued.

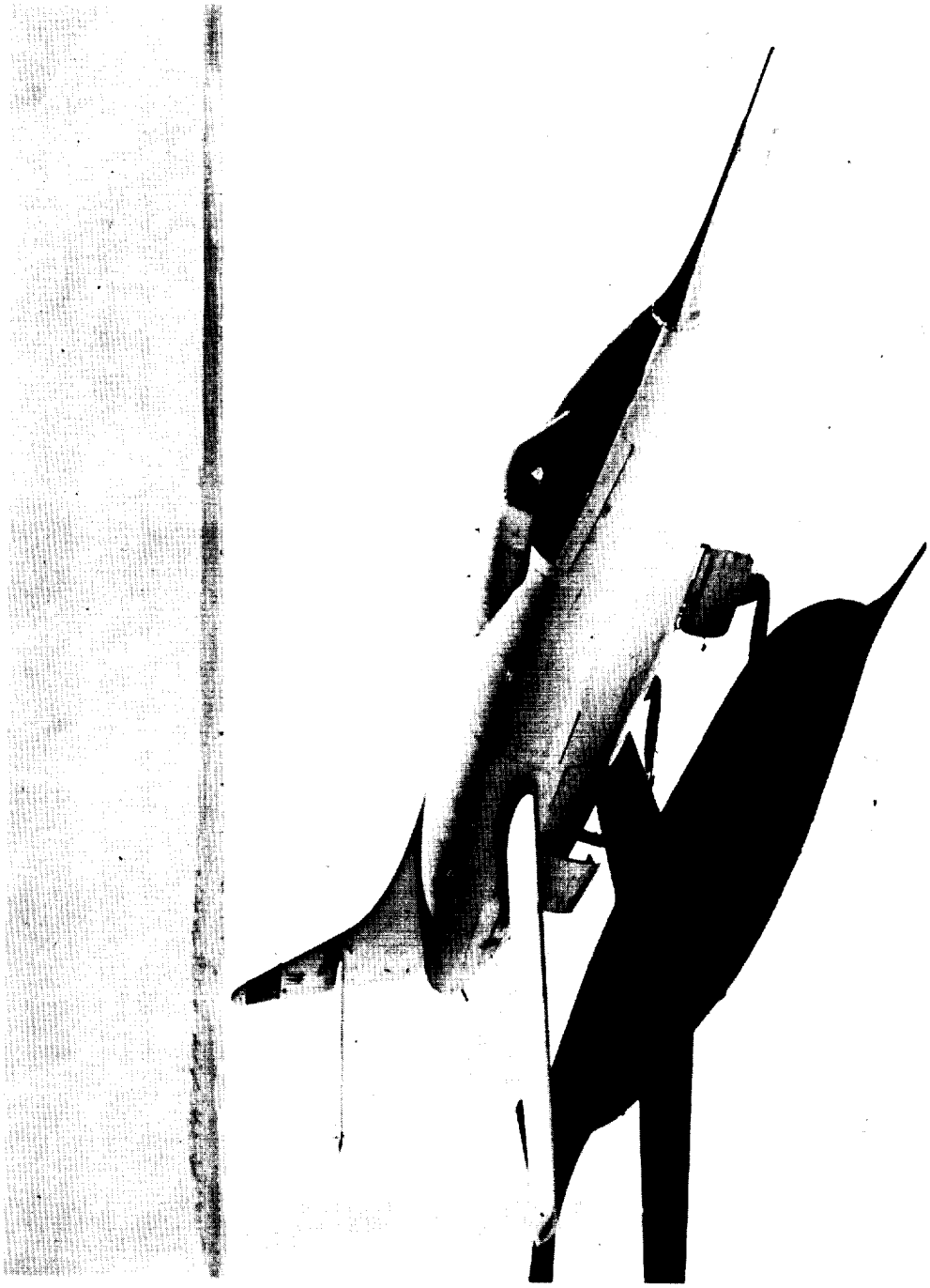

(d) D-558-II airplane. E-1438

Figure 2.- Continued.

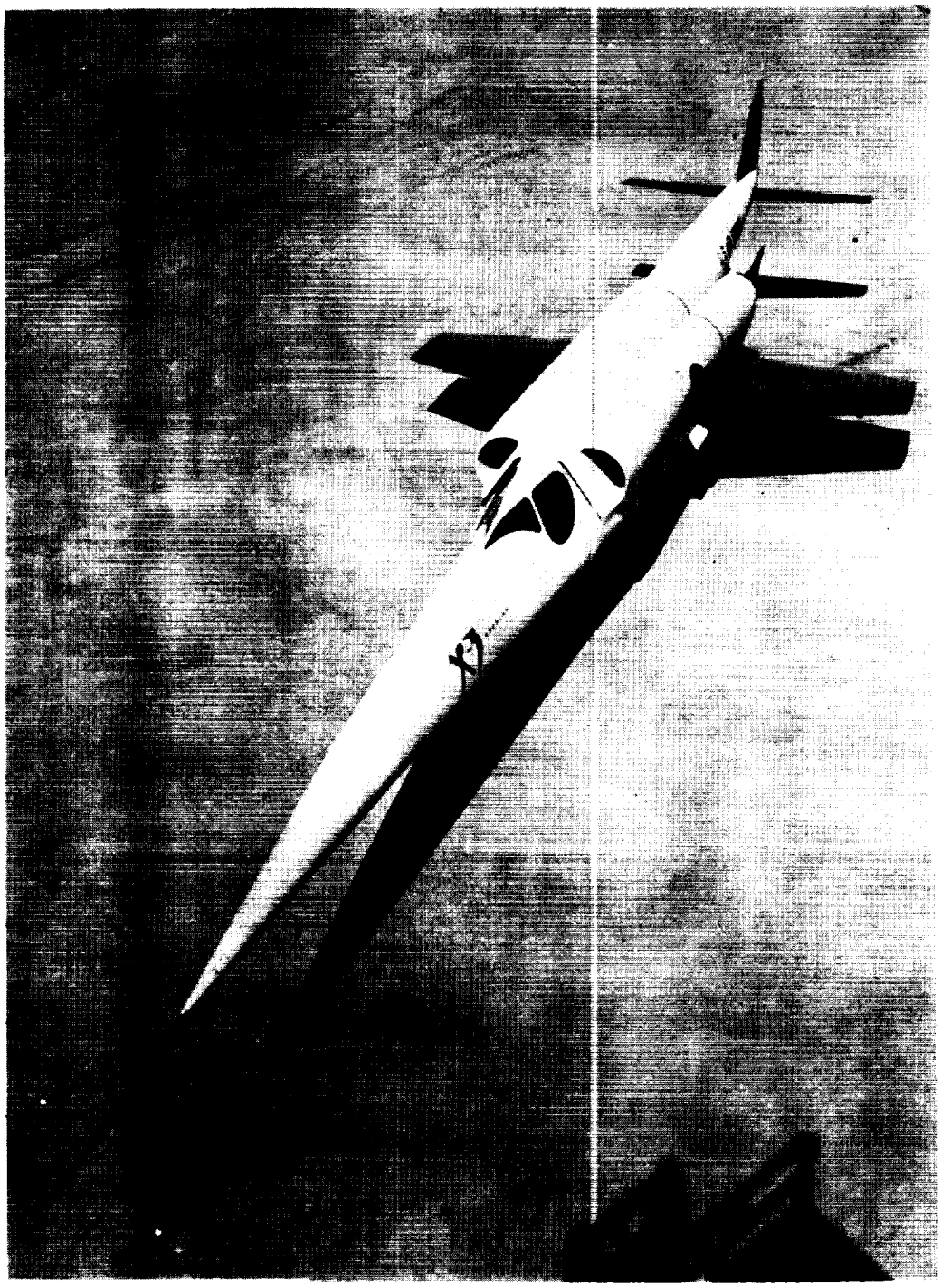

(e) X-3 airplane. E-1228

Figure 2.- Continued.

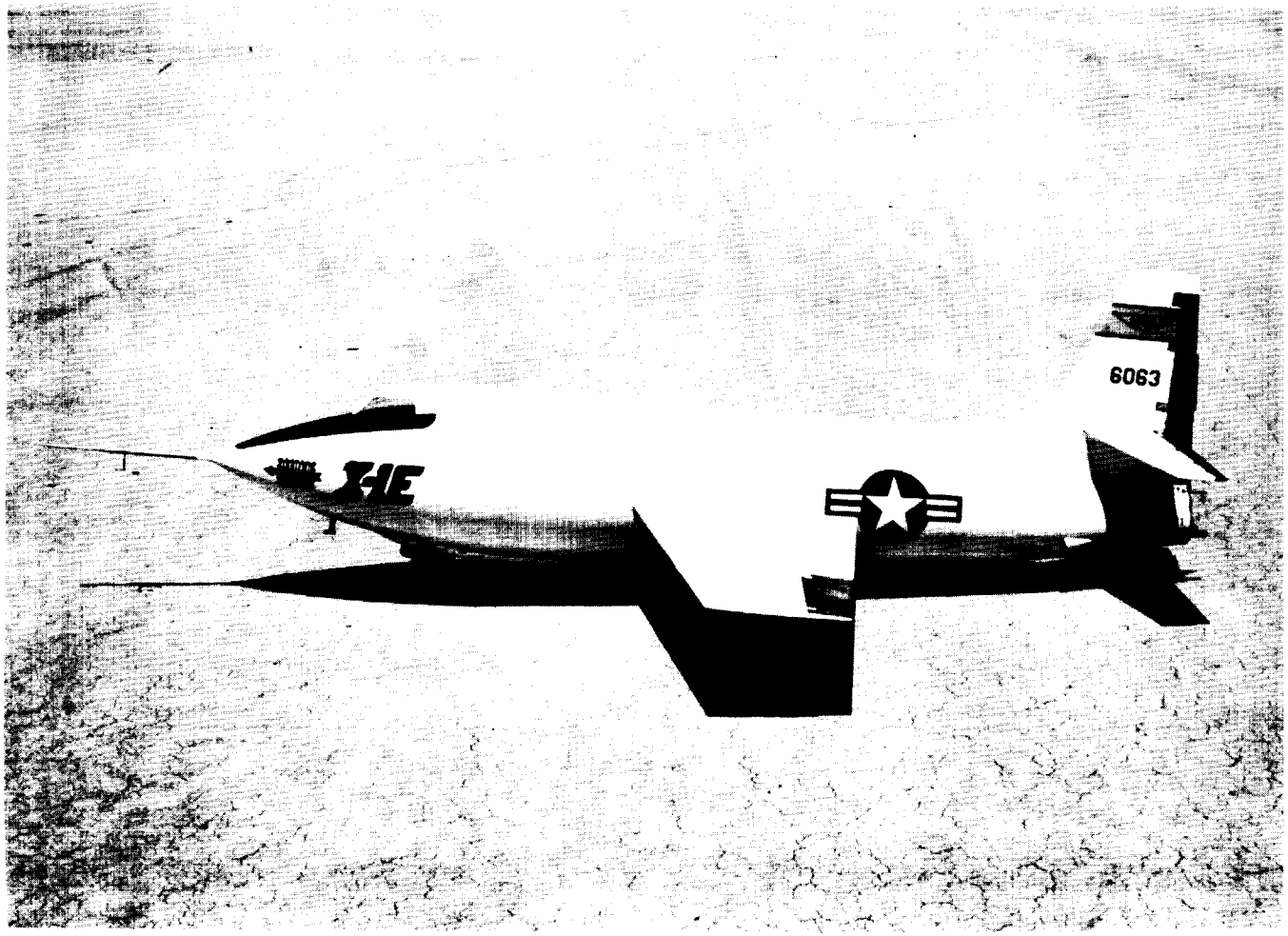

(f) X-1E airplane. E-1925

Figure 2.- Concluded.

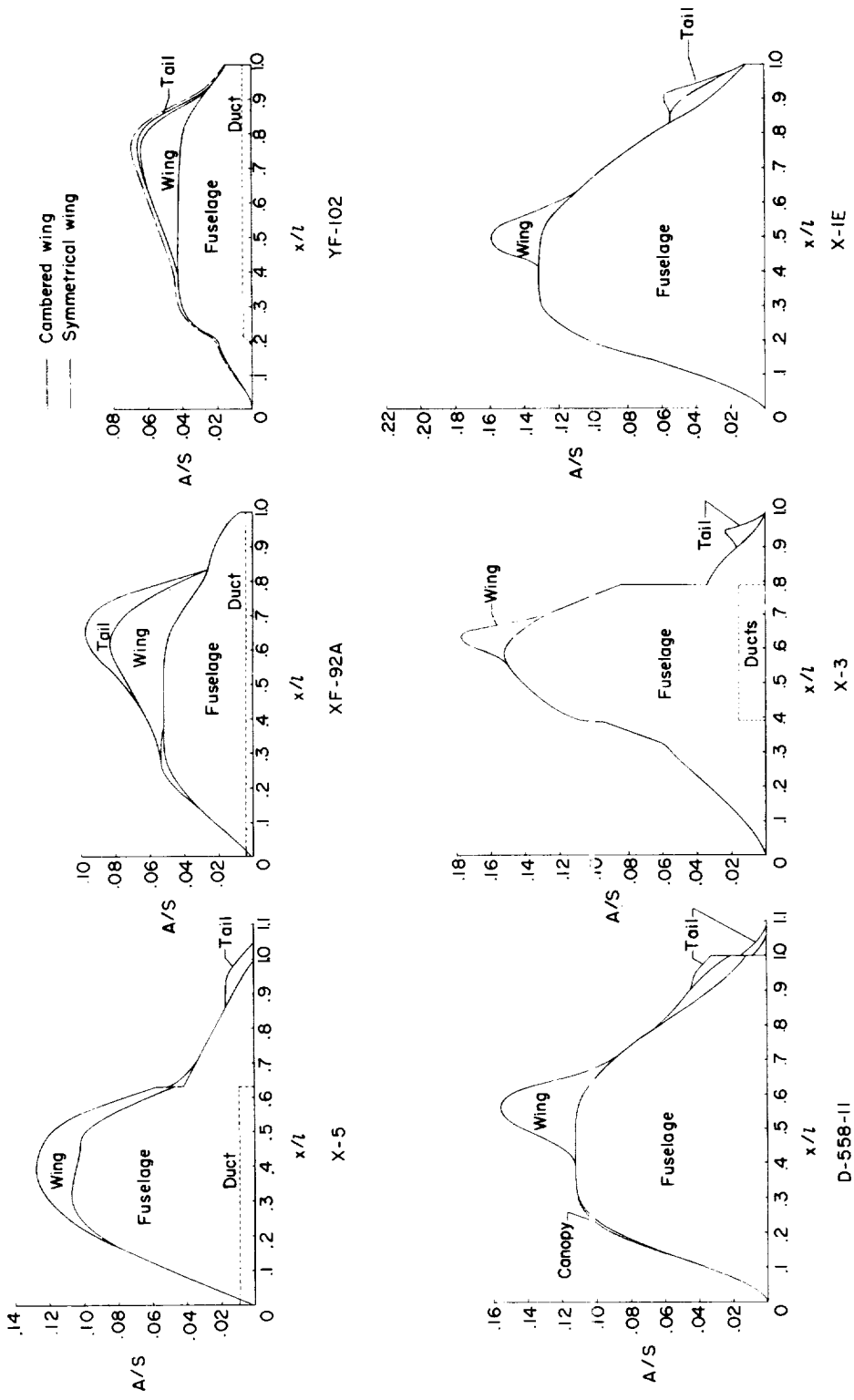

Figure 3.- Comparison of the cross-sectional area distributions of the airplanes.

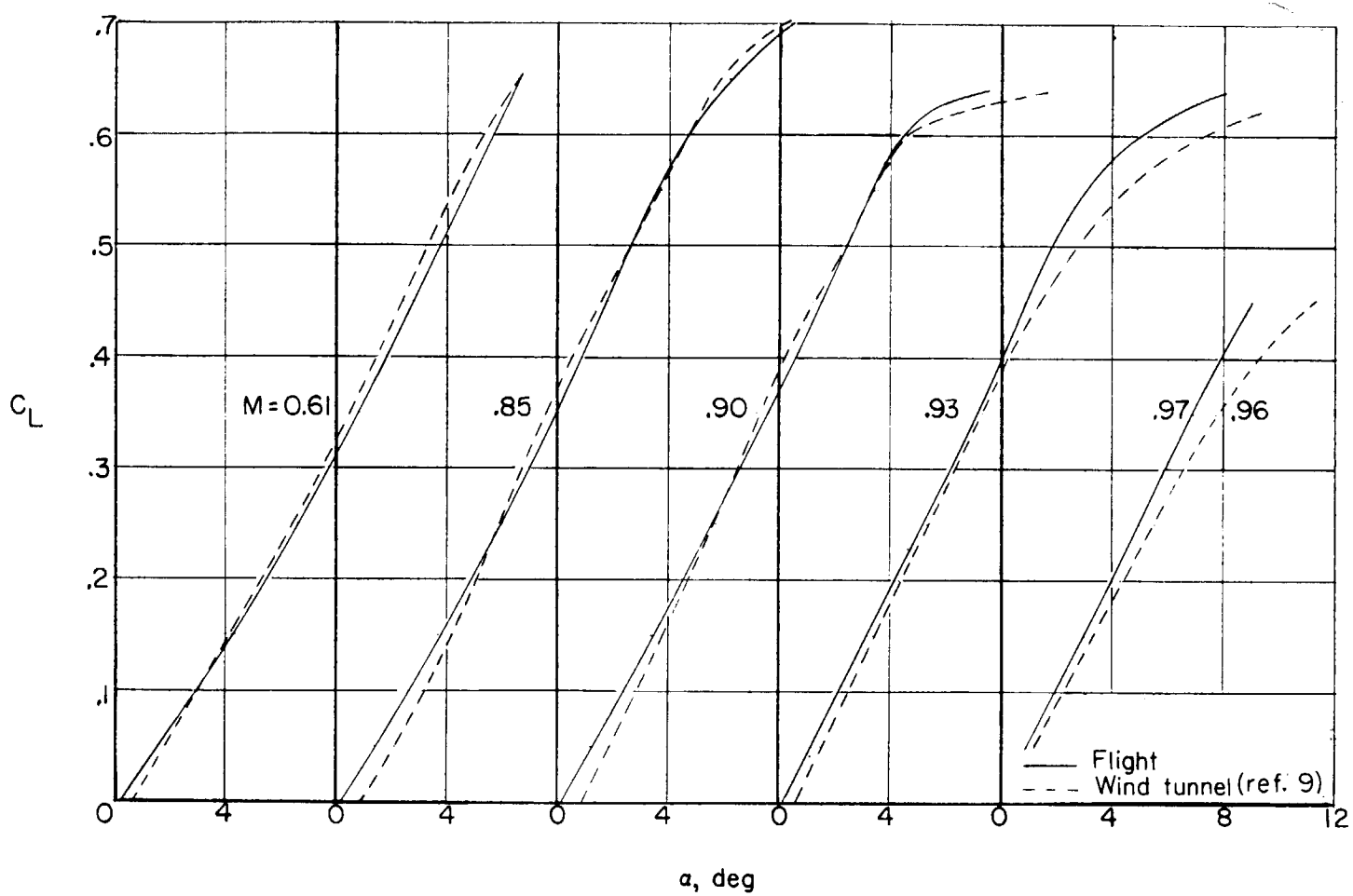

(a) X-5 airplane.

Figure 4.- Variation of lift coefficient with angle of attack for various constant Mach numbers showing comparison with wind-tunnel data.

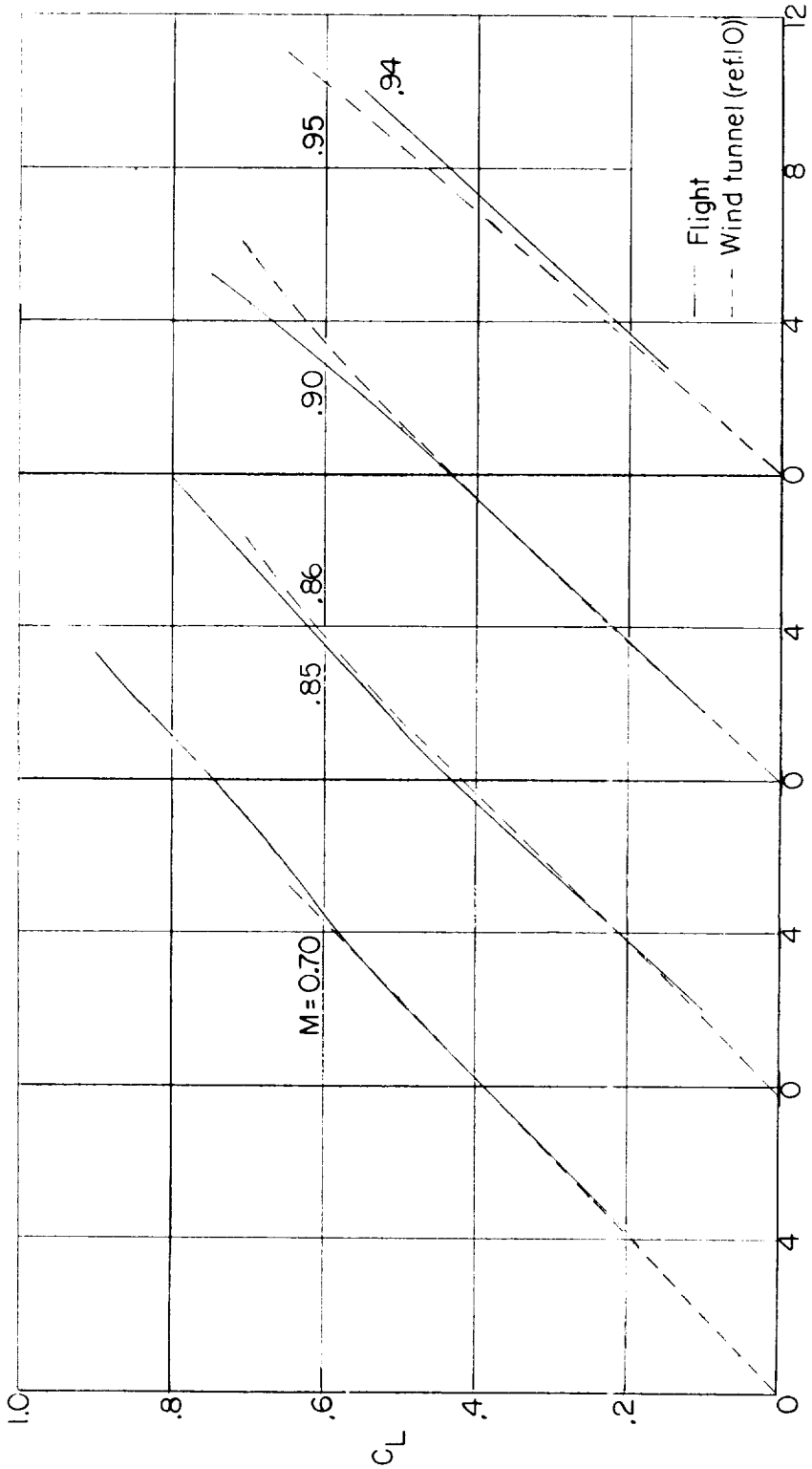

(b) XF-92A airplane.

Figure 4.- Continued.

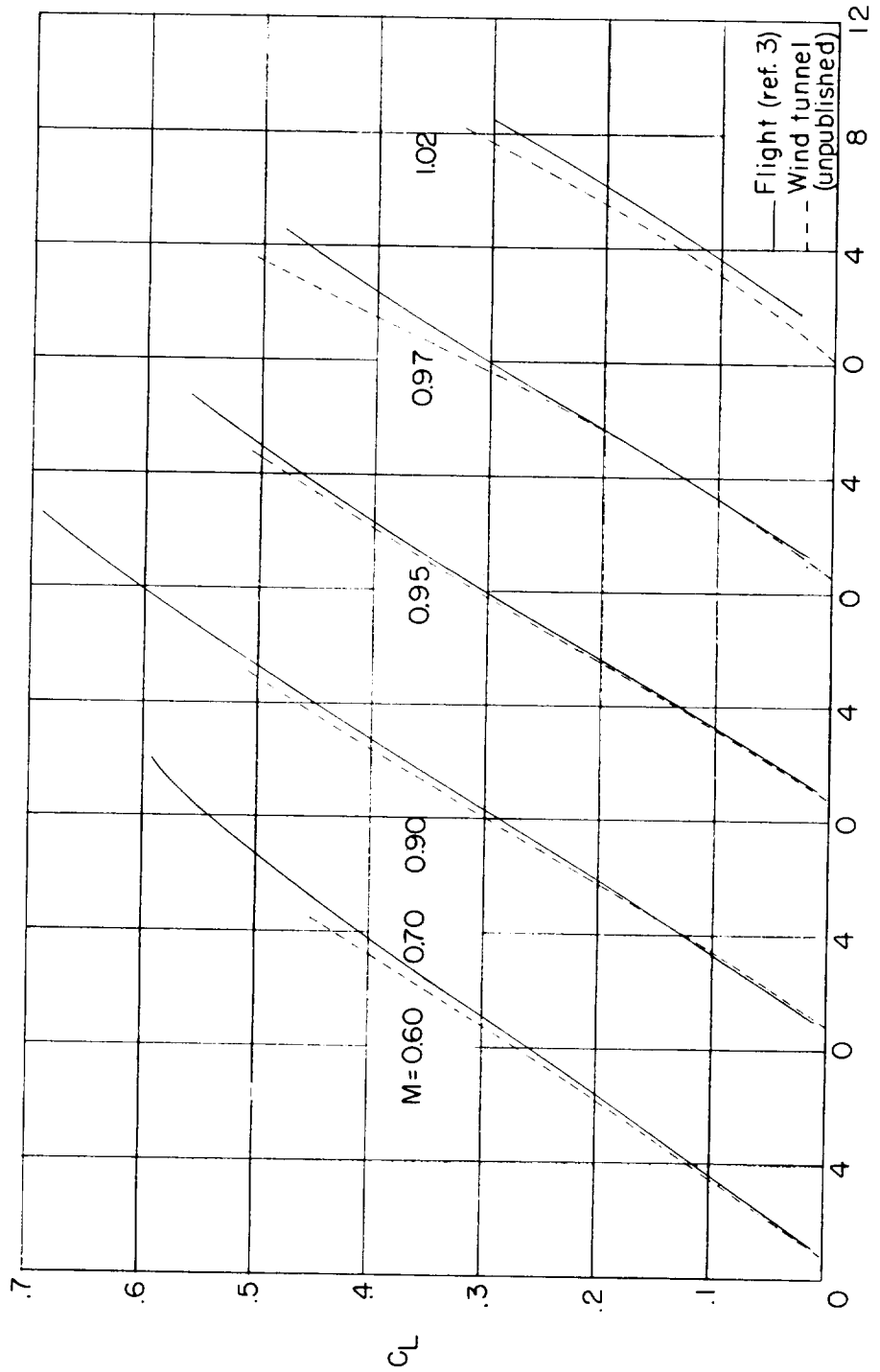

(c) YF-102 (cambered wing) airplane.

Figure 4.- Continued.

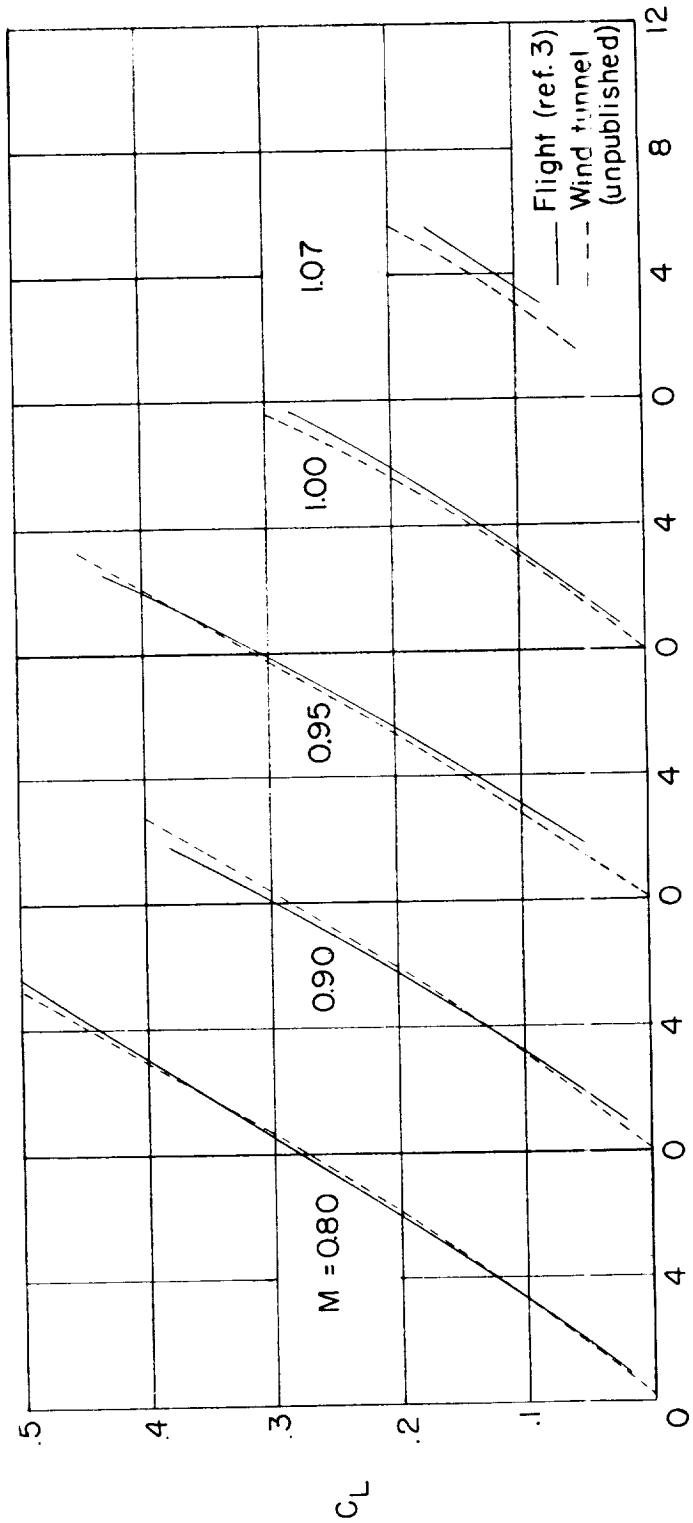

(d) YF-102 (symmetrical wing) airplane.

Figure 4.- Continued.

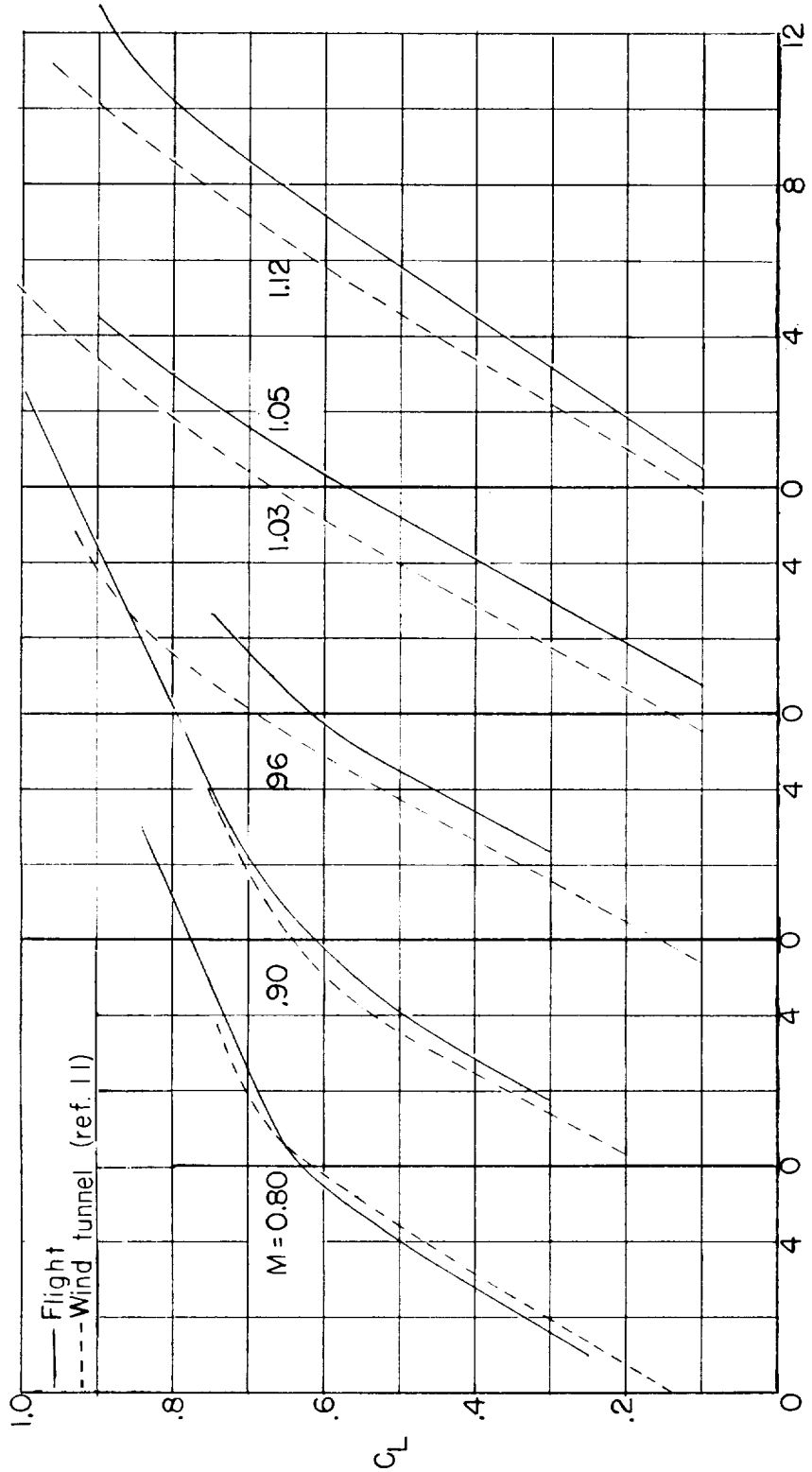

(e) D-558-II airplane.

Figure 4.- Continued.

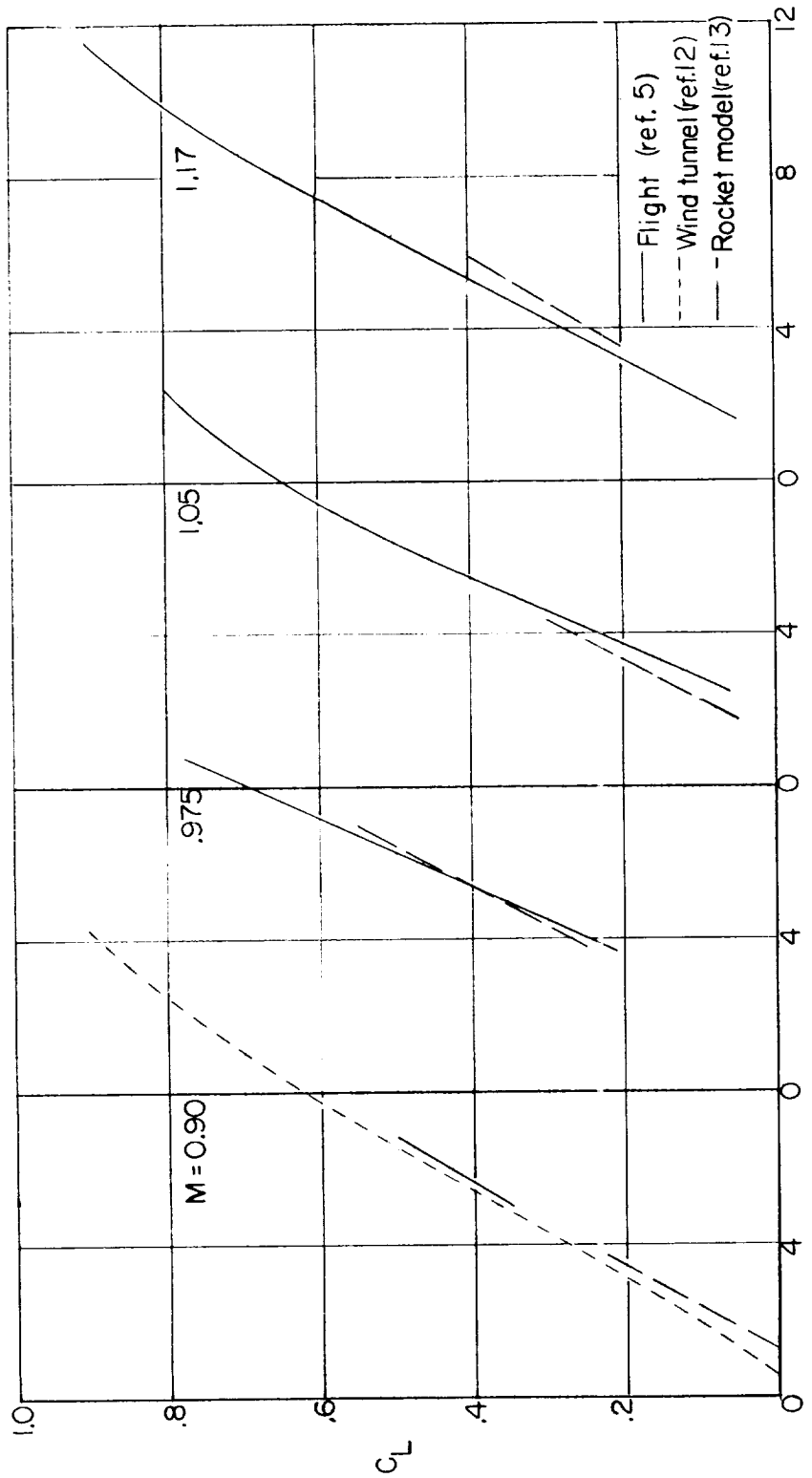

(f) X-3 airplane.

Figure 4.- Continued.

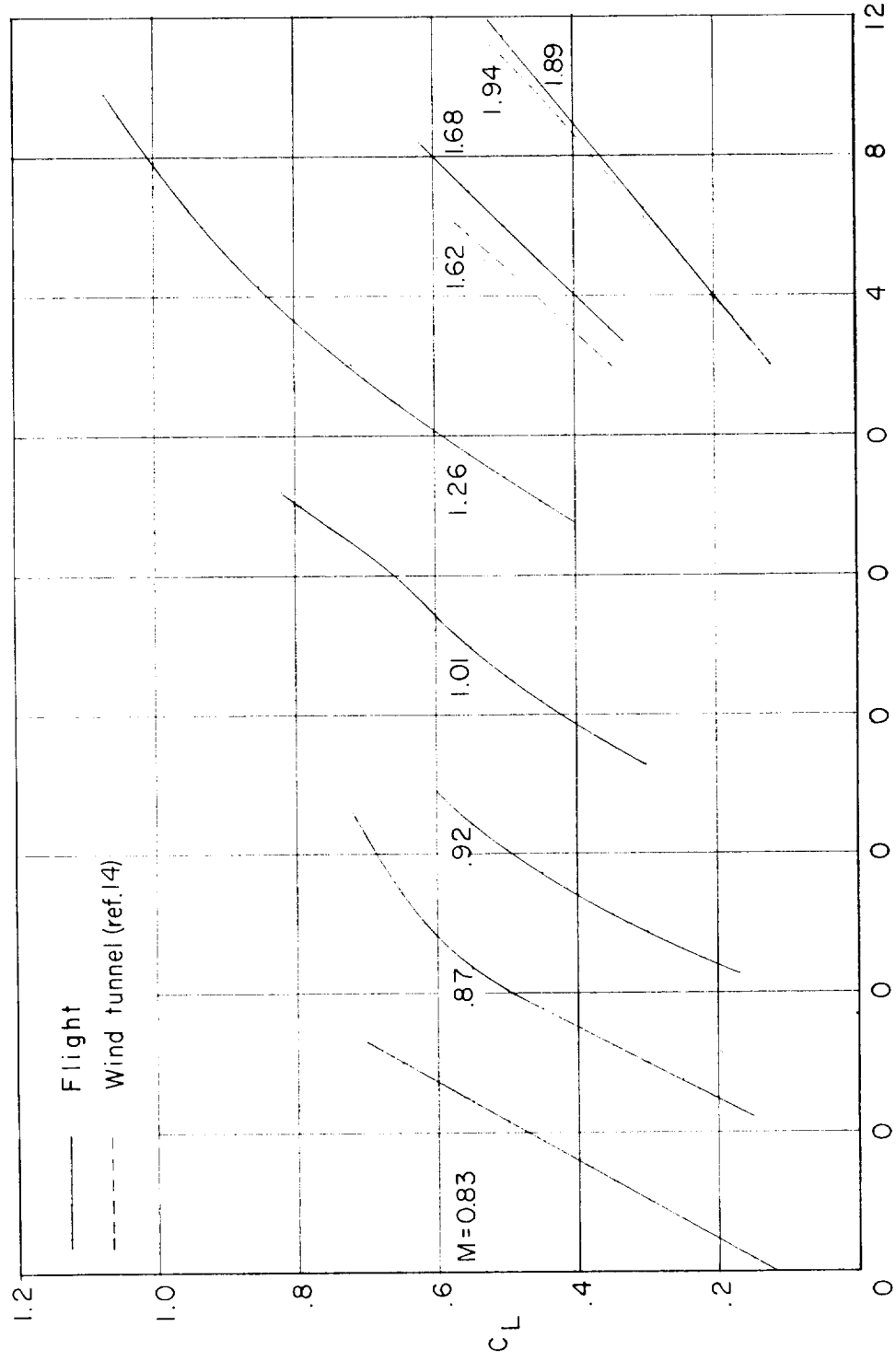

(g) X-1E airplane.

Figure 4.- Concluded.

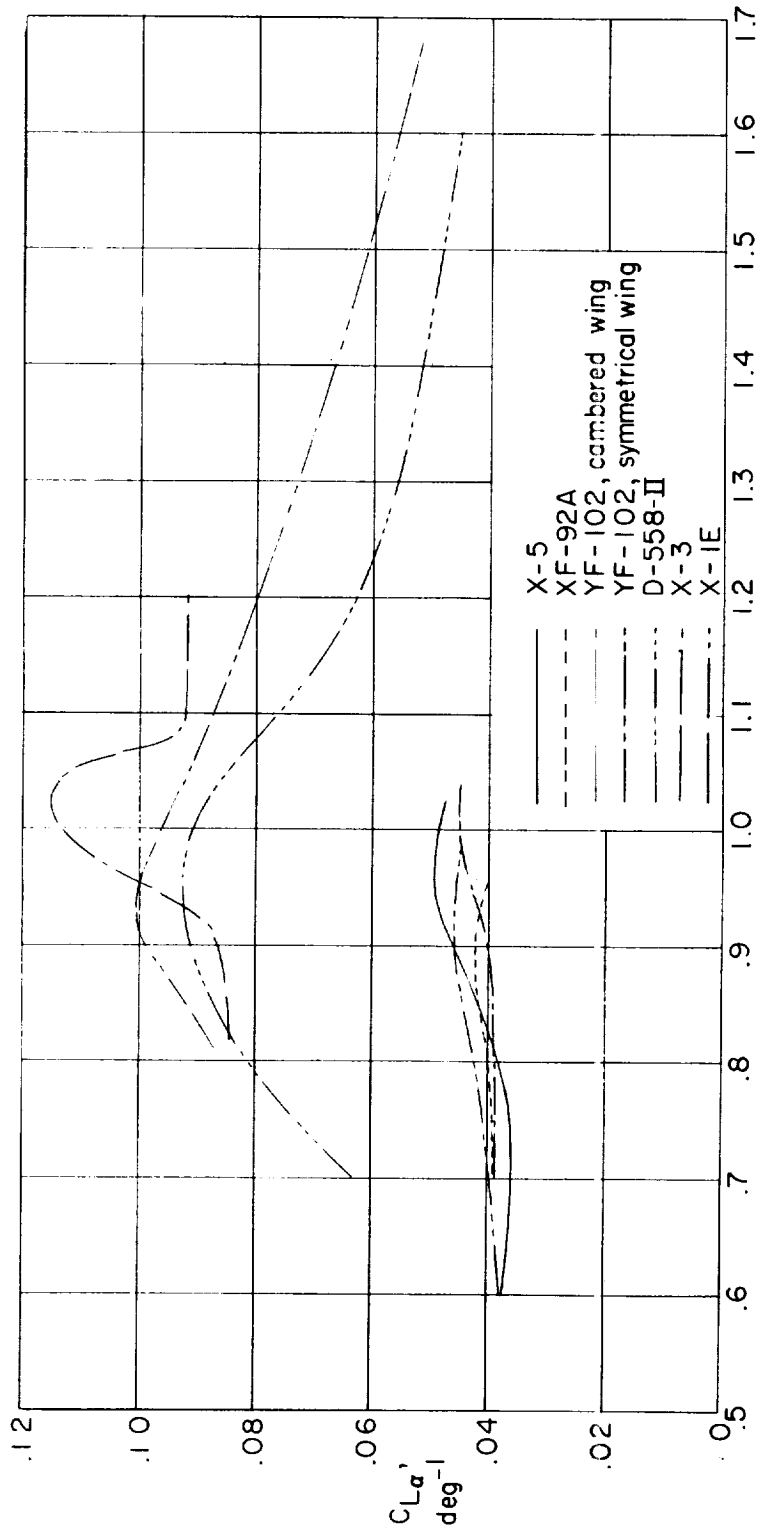

Figure 5.- Variation of lift-curve slopes with Mach number. $C_L \approx 0.3$.

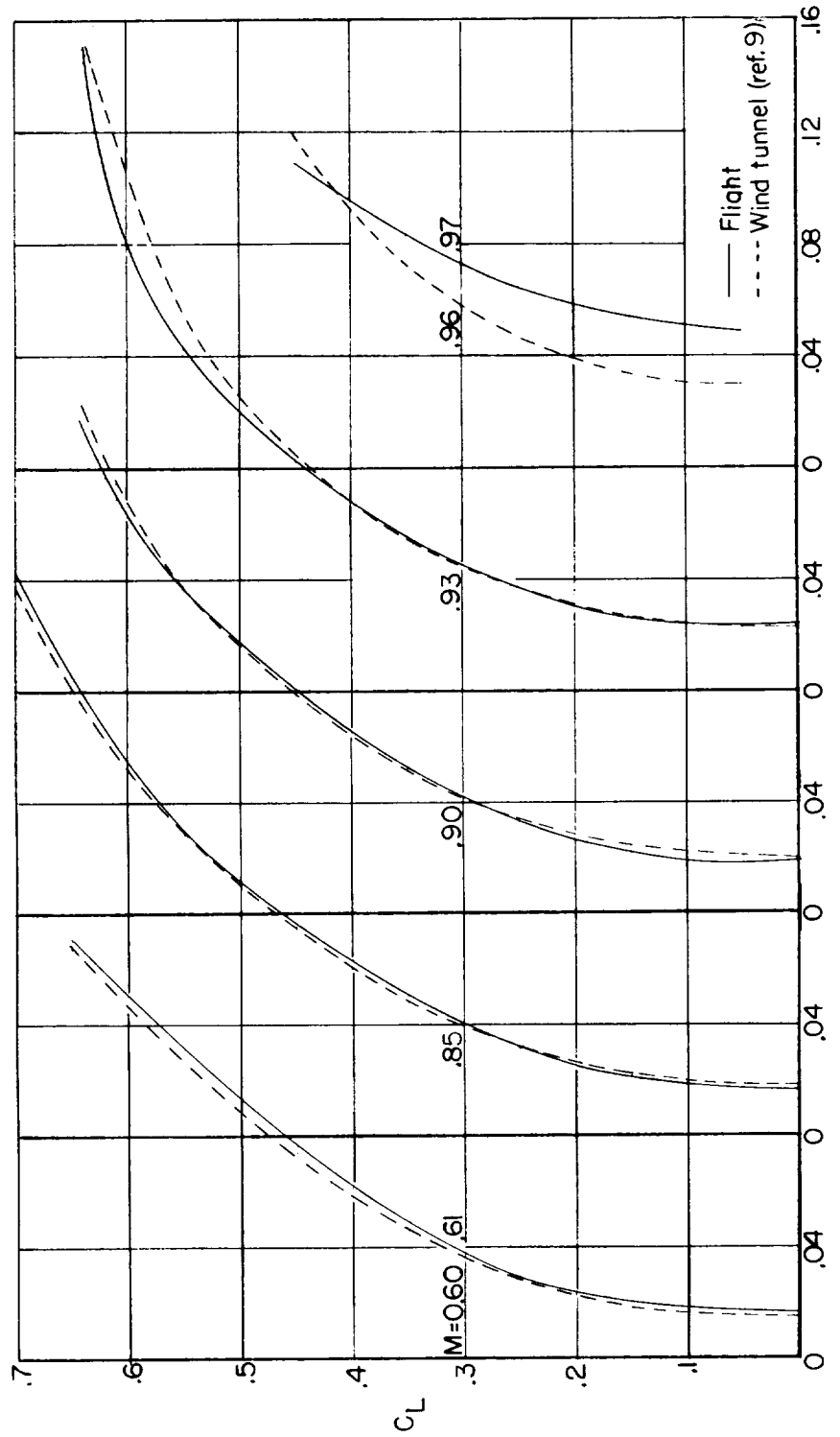

(a) X-5 airplane.

Figure 6.- Variation of drag coefficient with lift coefficient for various constant Mach numbers showing comparison with wind-tunnel data where available.

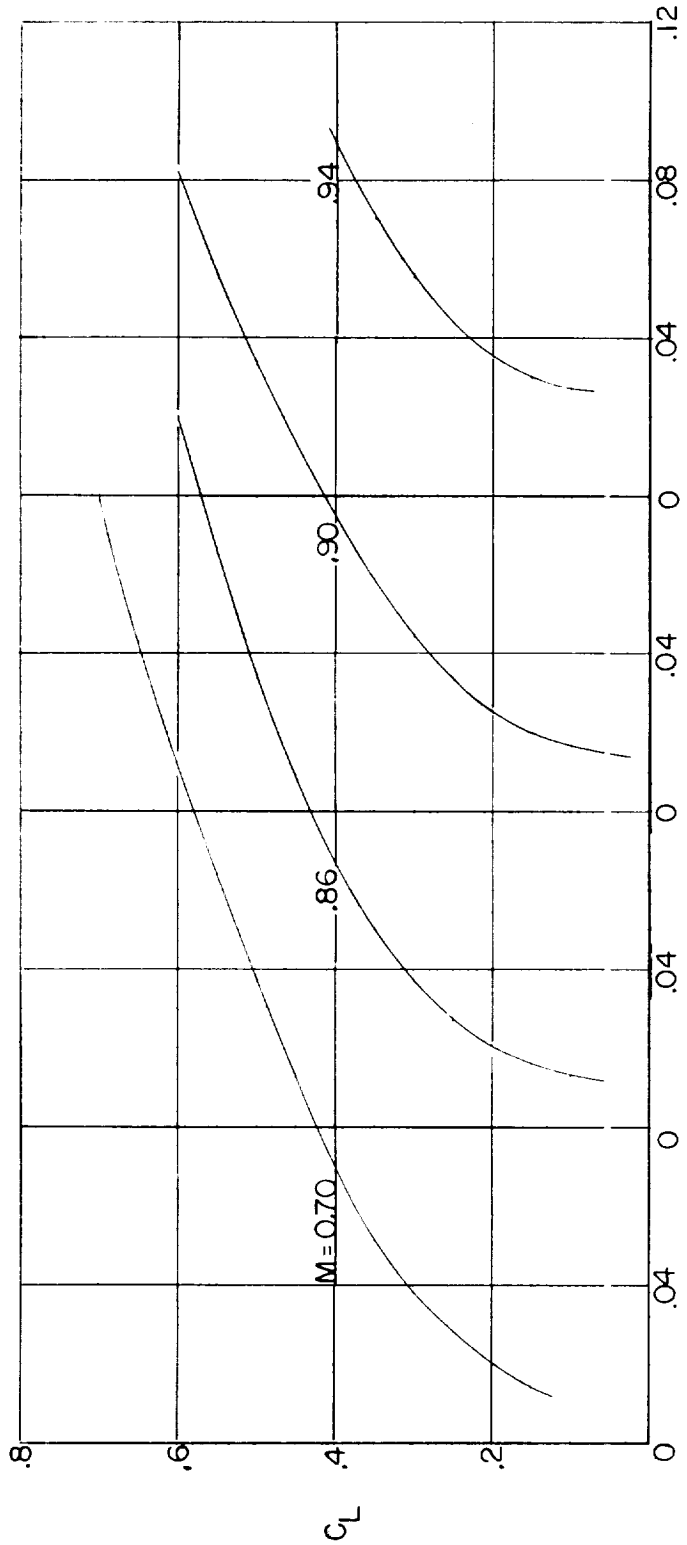

(b) XF-92A airplane.

Figure 6.- Continued.

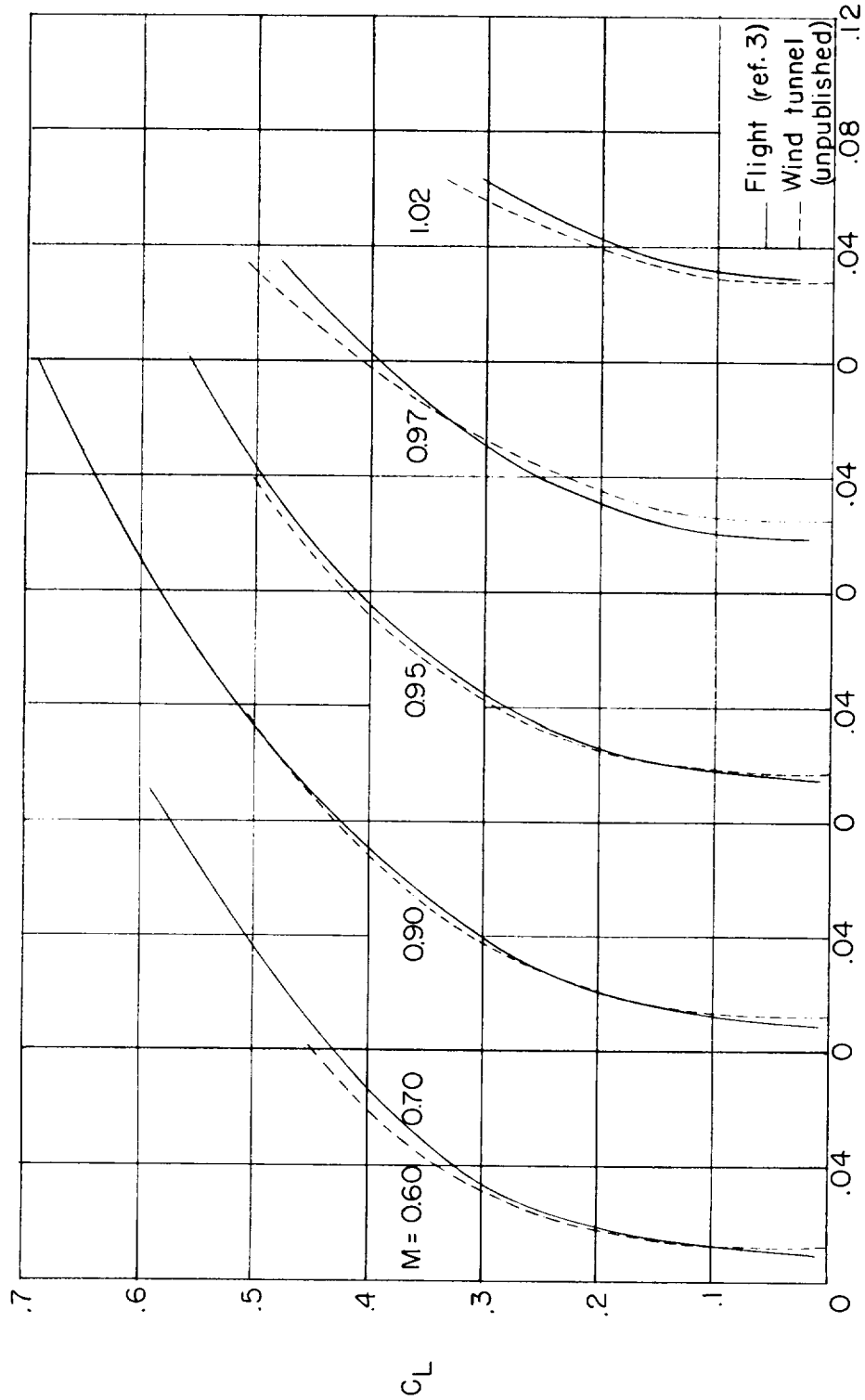

(c) YF-102 (cambered wing) airplane.

Figure 6.- Continued.

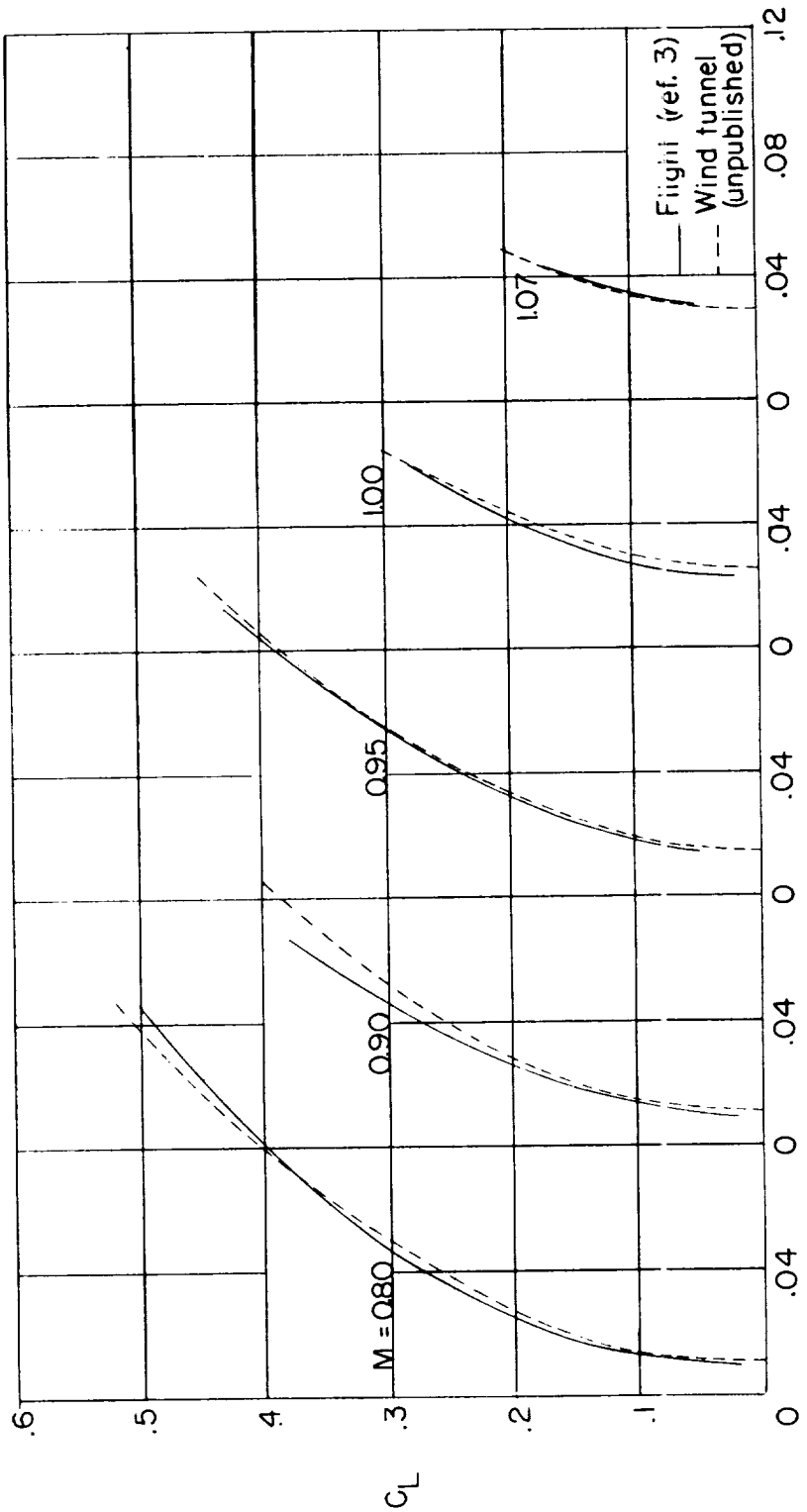

(d) YF-102 (symmetrical wing) airplane.

Figure 6.- Continued.

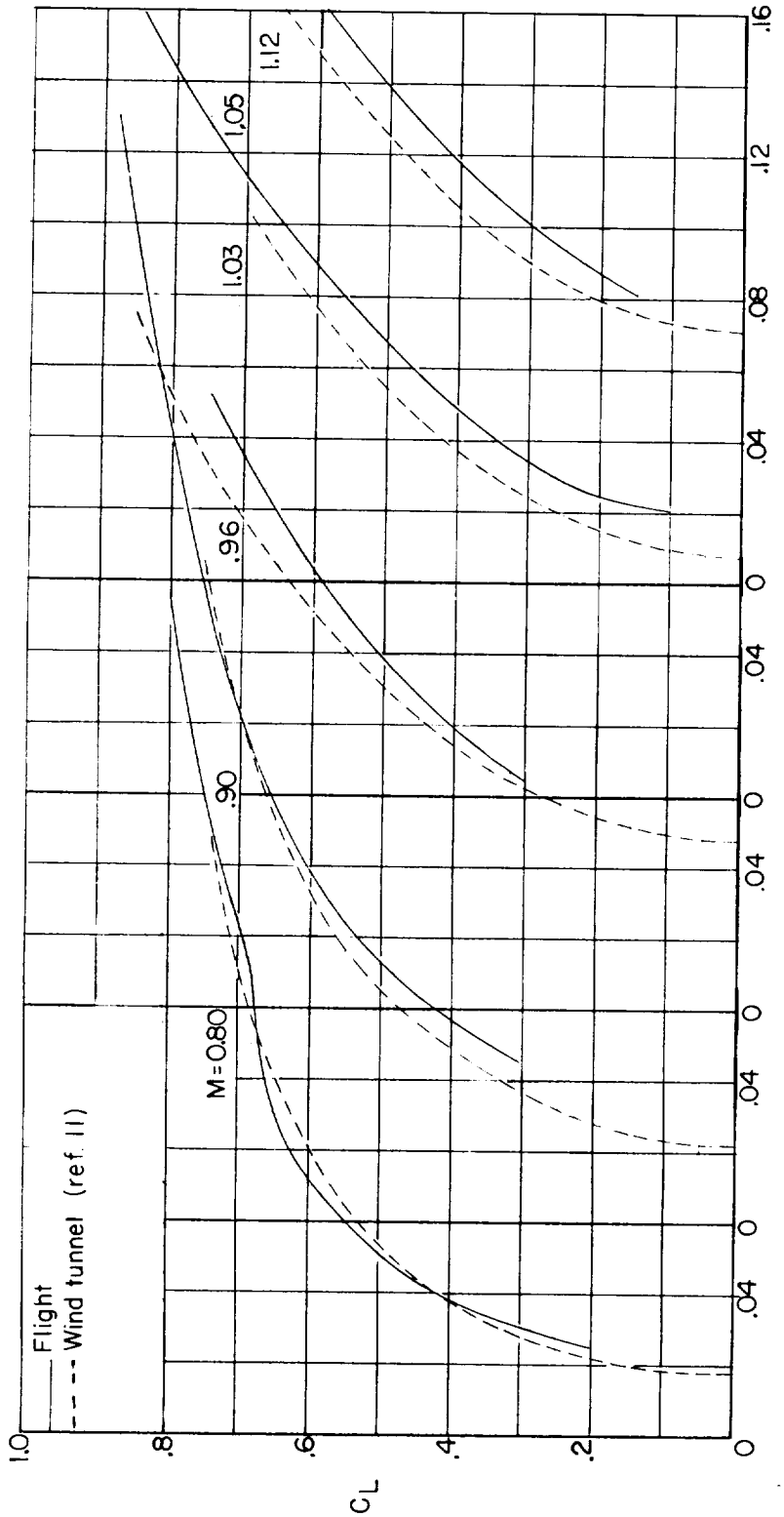

(e) D-558-II airplane.

Figure 6.- Continued.

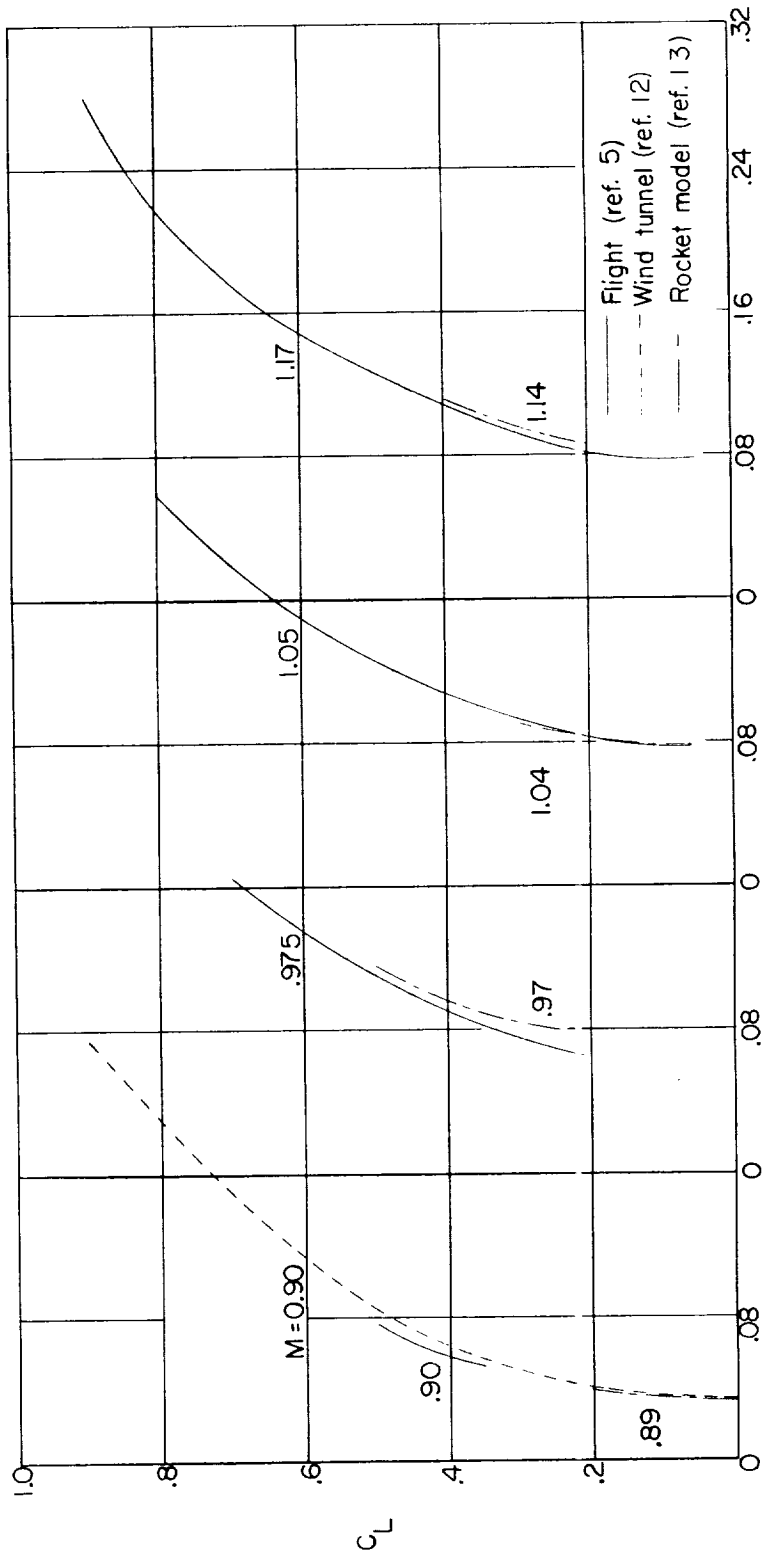

(f) X-3 airplane.

Figure 6.- Continued.

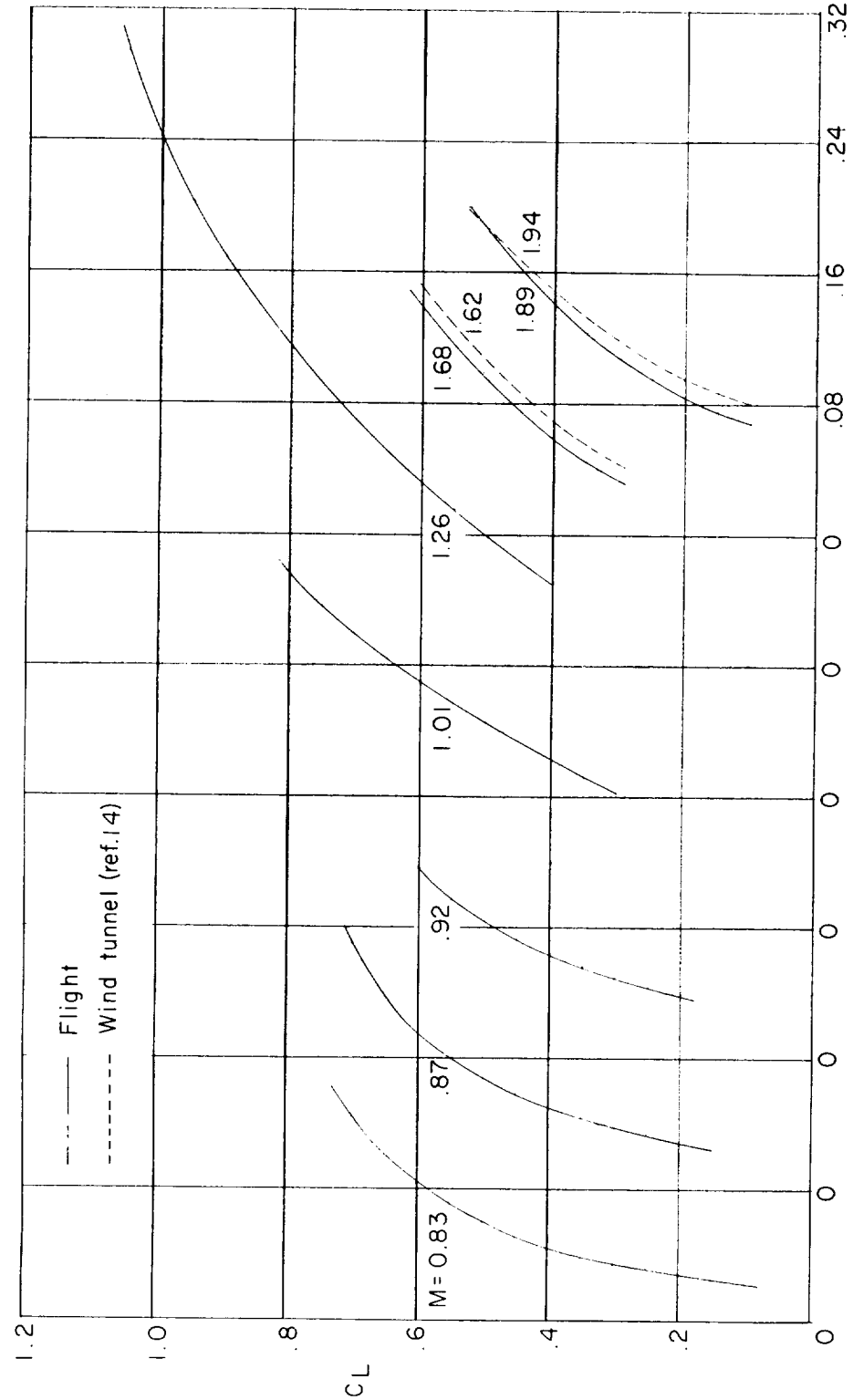

(g) X-1E airplane.

Figure 6.- Concluded.

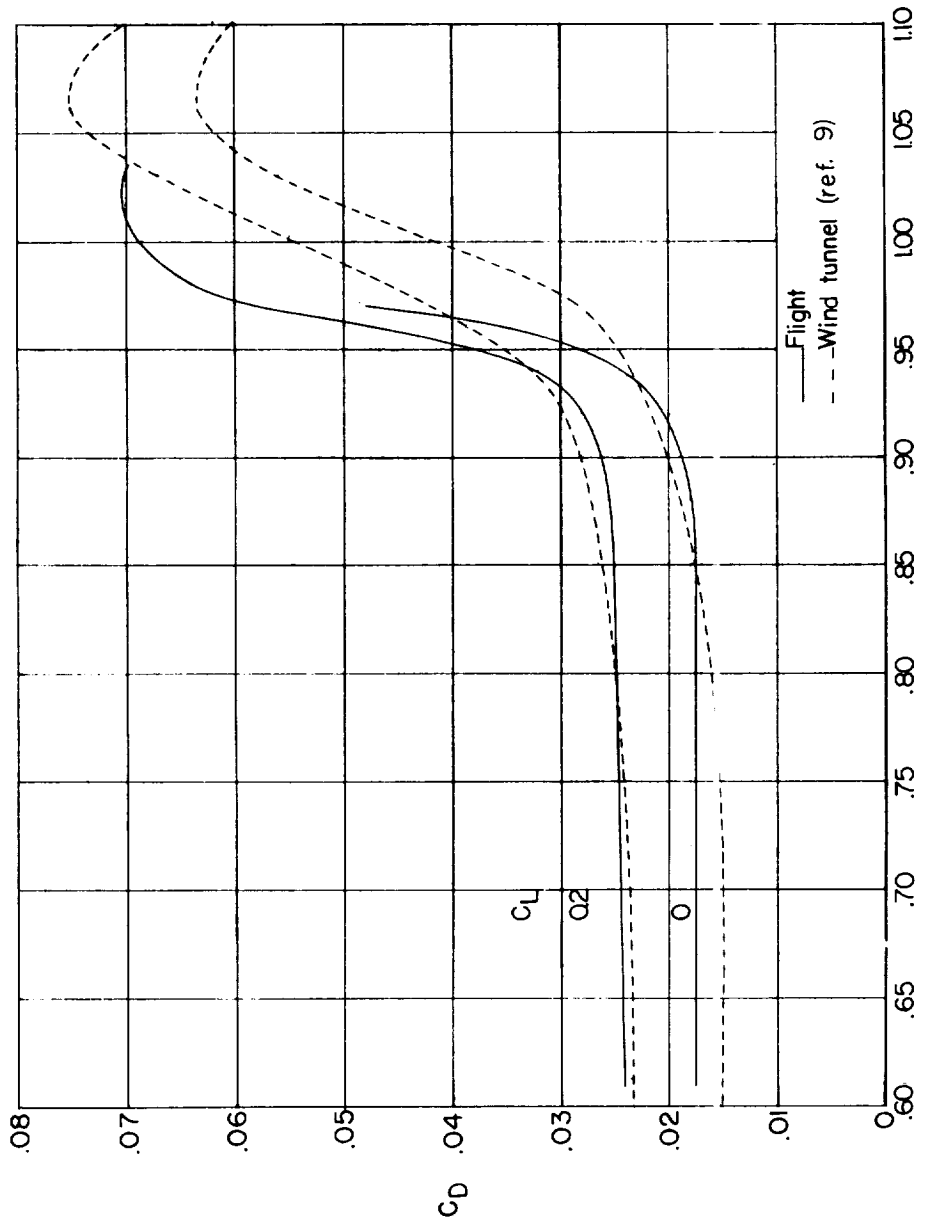

(a) X-5 airplane.

Figure 7.- Variation of drag coefficient with Mach number for various constant lift coefficients showing comparison with wind-tunnel and rocket-model data.

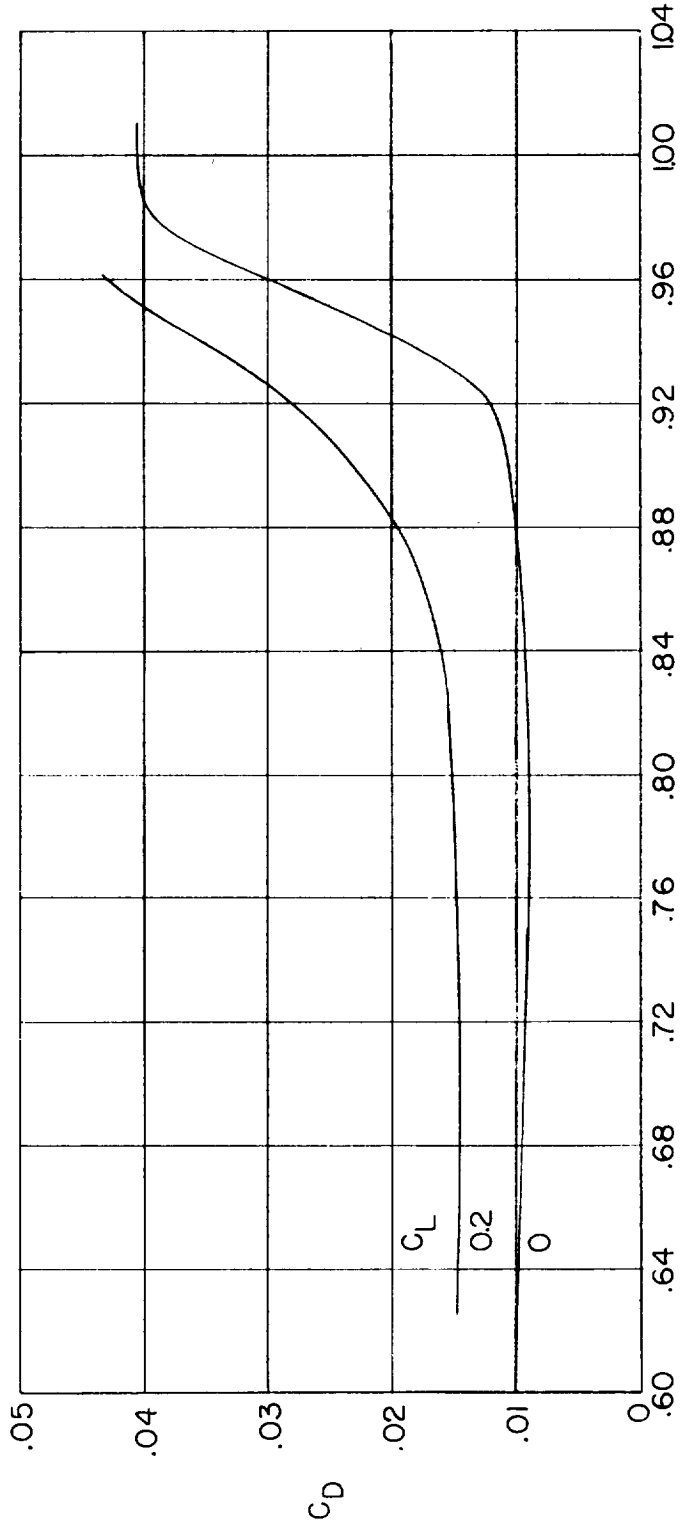

(b) XF-92A airplane.

Figure 7.- Continued.

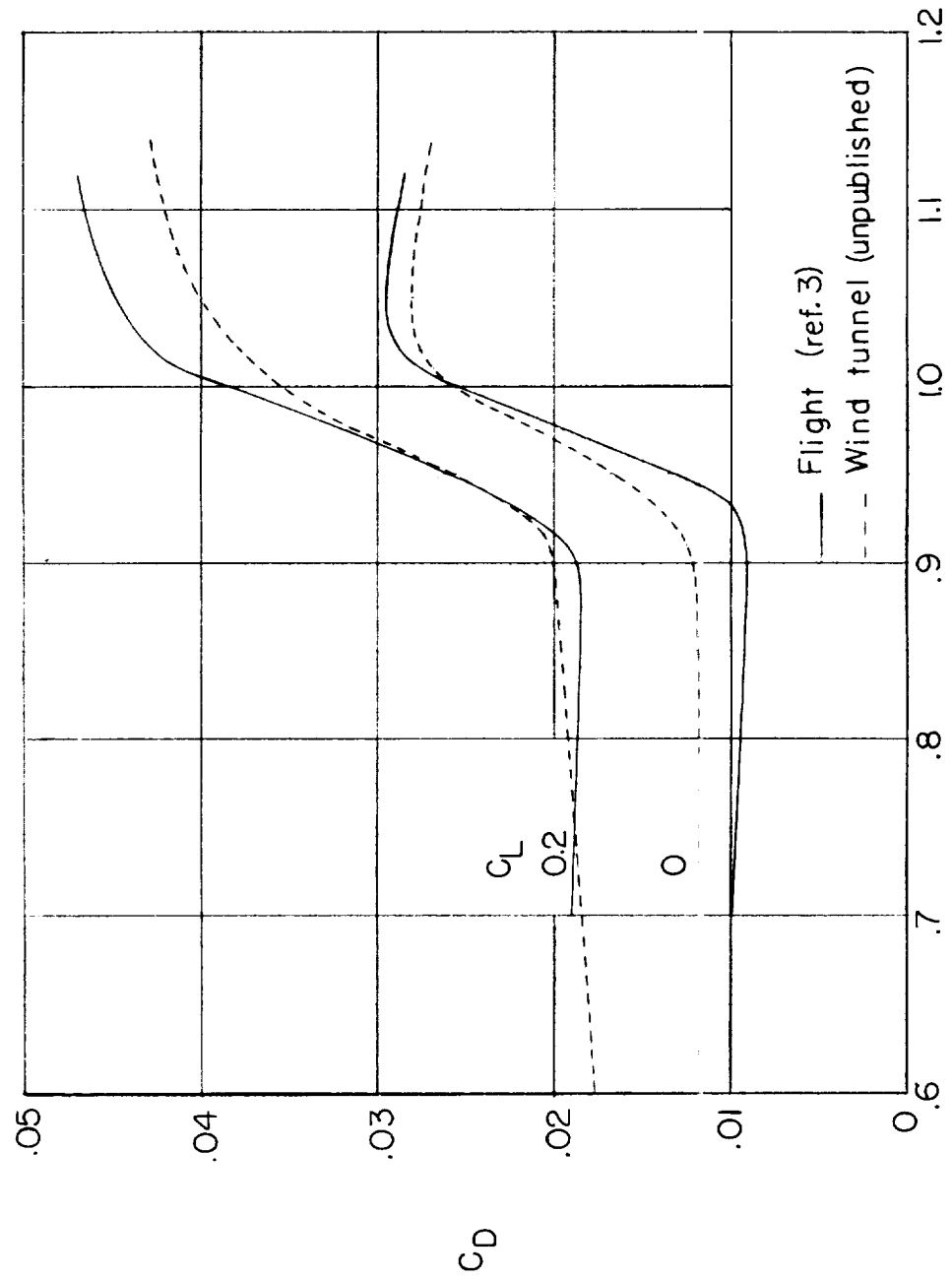

(c) YF-102 (cambered wing) airplane.

Figure 7.- Continued.

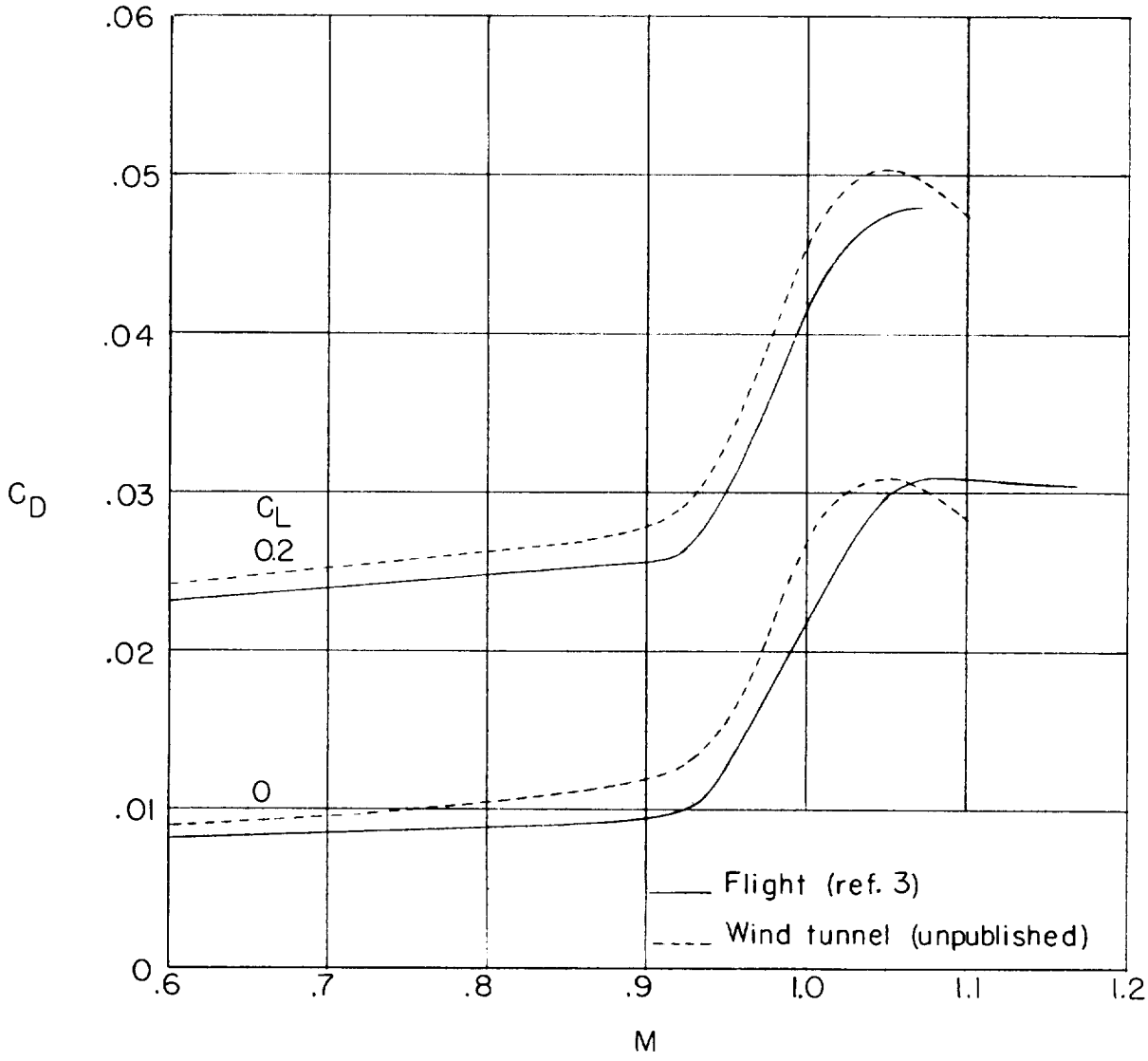

(d) YF-102 (symmetrical wing) airplane.

Figure 7.- Continued.

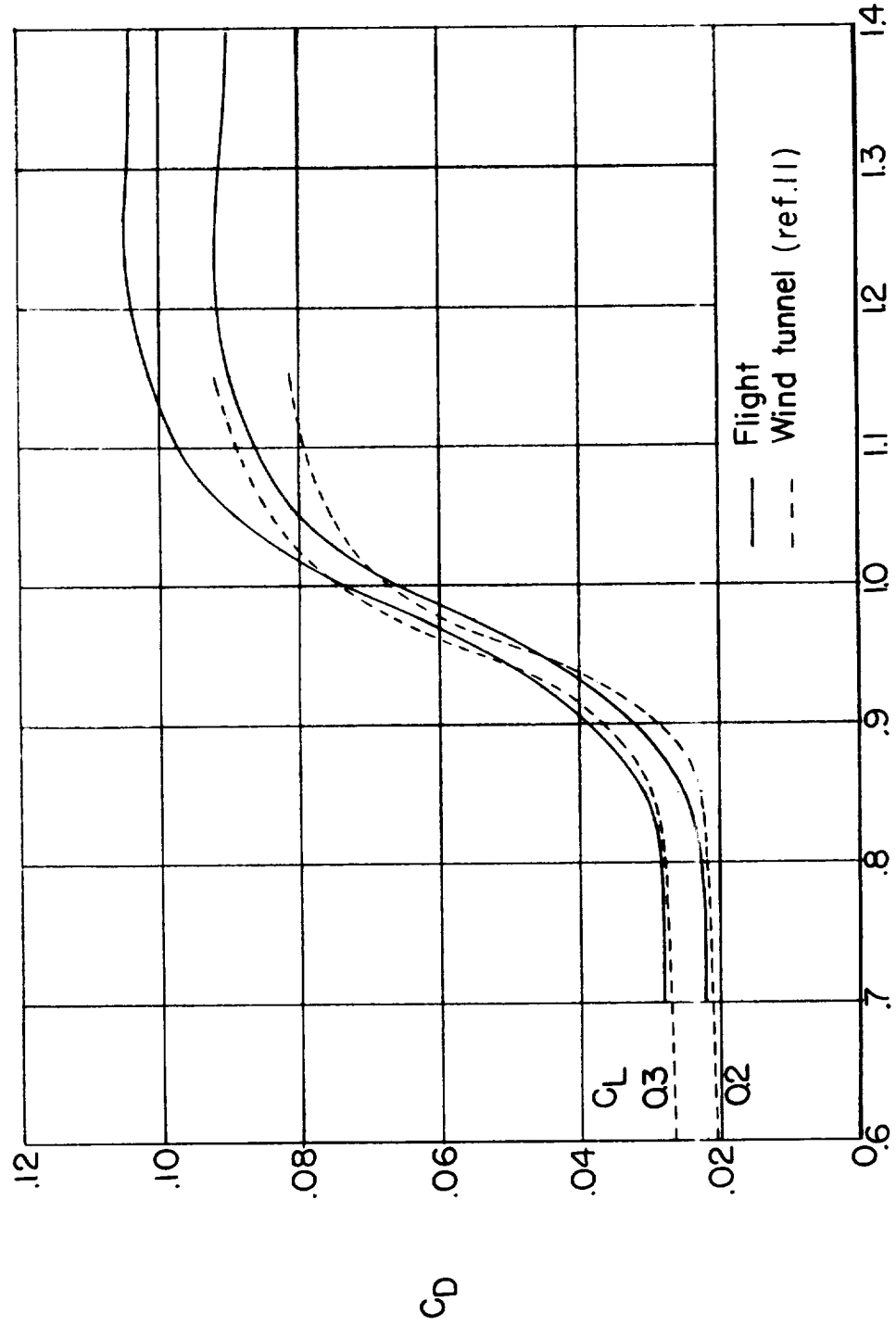

(e) D-558-II airplane.

Figure 7.- Continued.

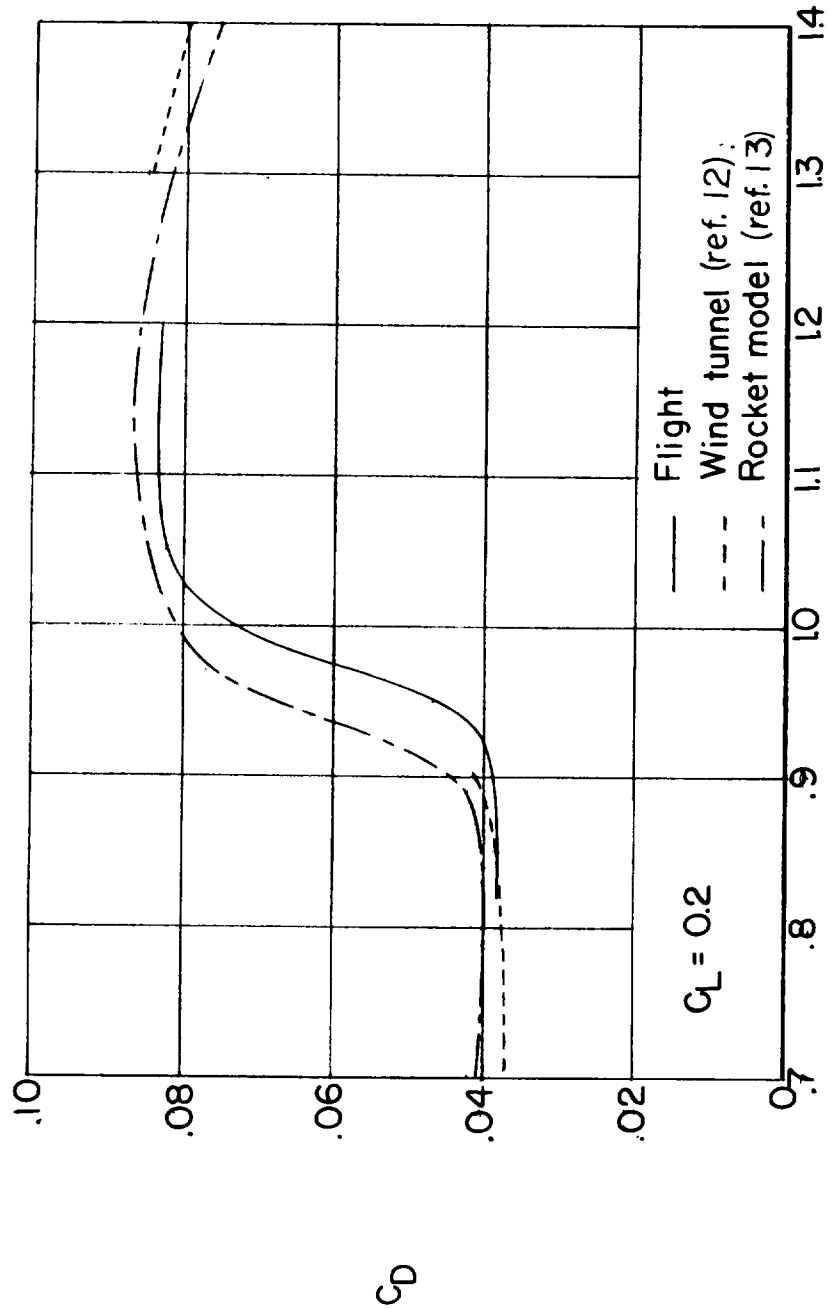

(f) X-3 airplane.

Figure 7.- Continued.

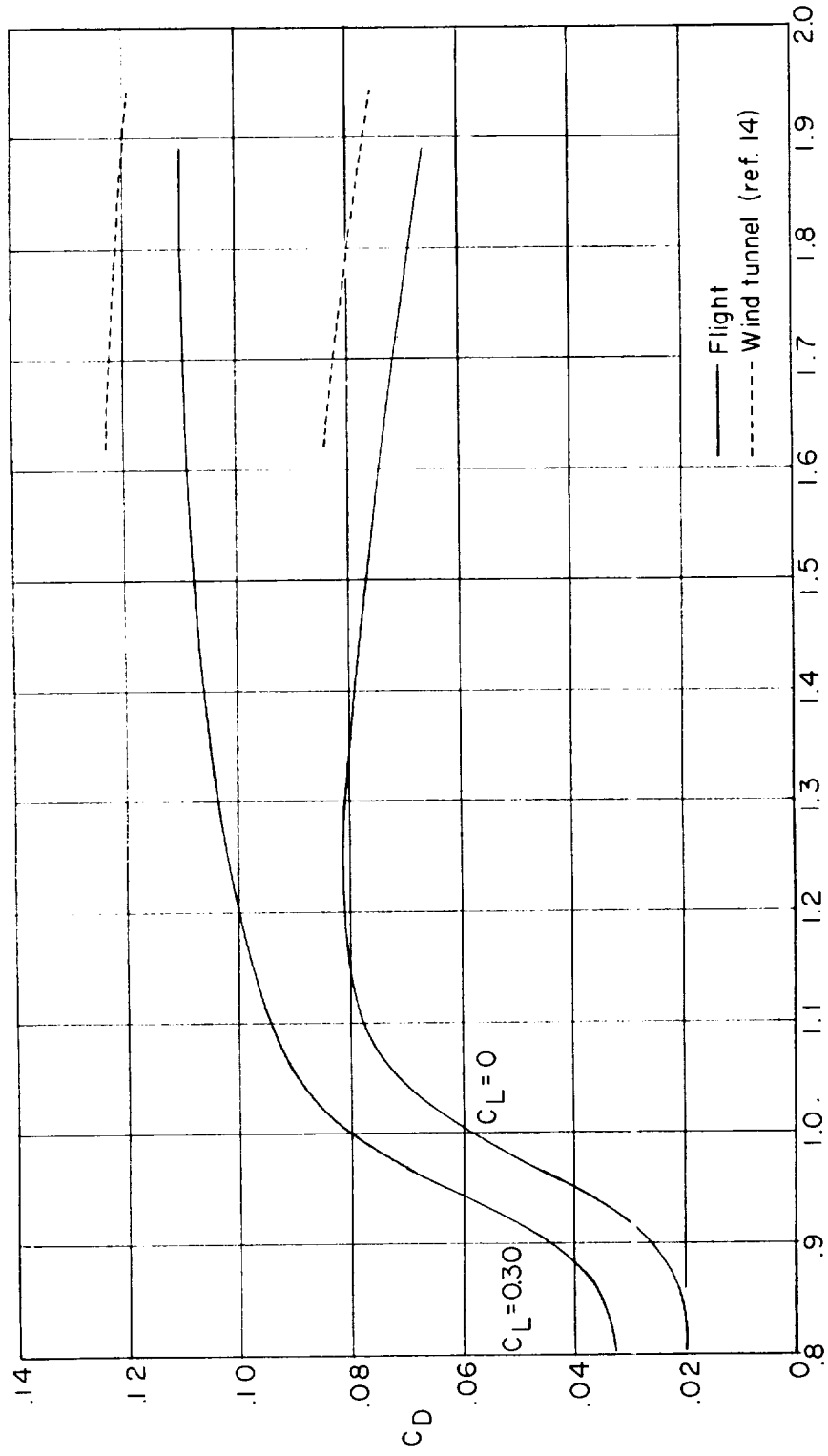

(g) X-1E airplane.

Figure 7.- Concluded.

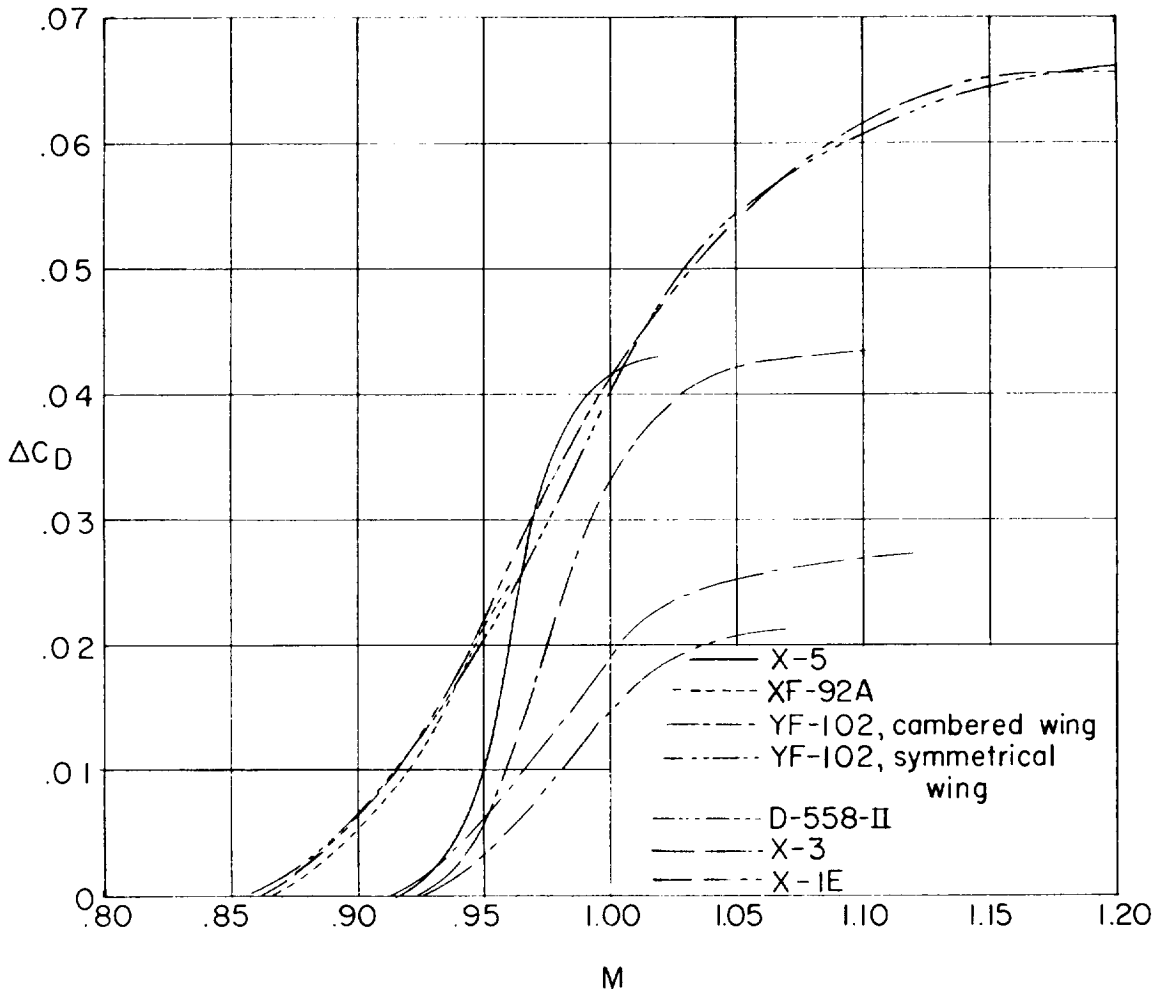

Figure 8.- Variation with Mach number of the drag-coefficient increment above the drag-rise Mach number. $C_L = 0.2$.

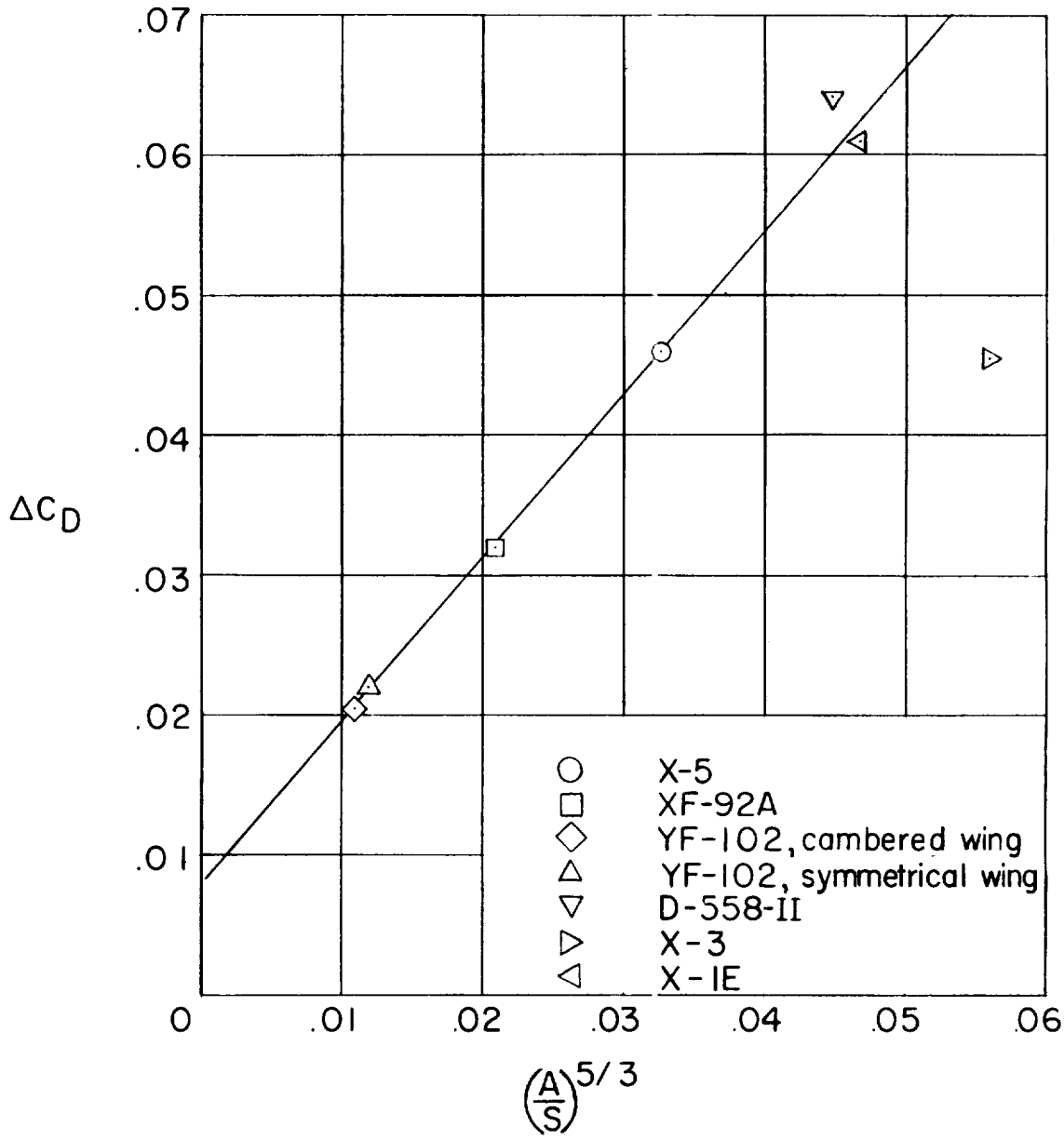

Figure 9.- Relationship between transonic drag-coefficient increment and ratio of maximum cross-sectional area to wing area. $C_L \approx 0$.

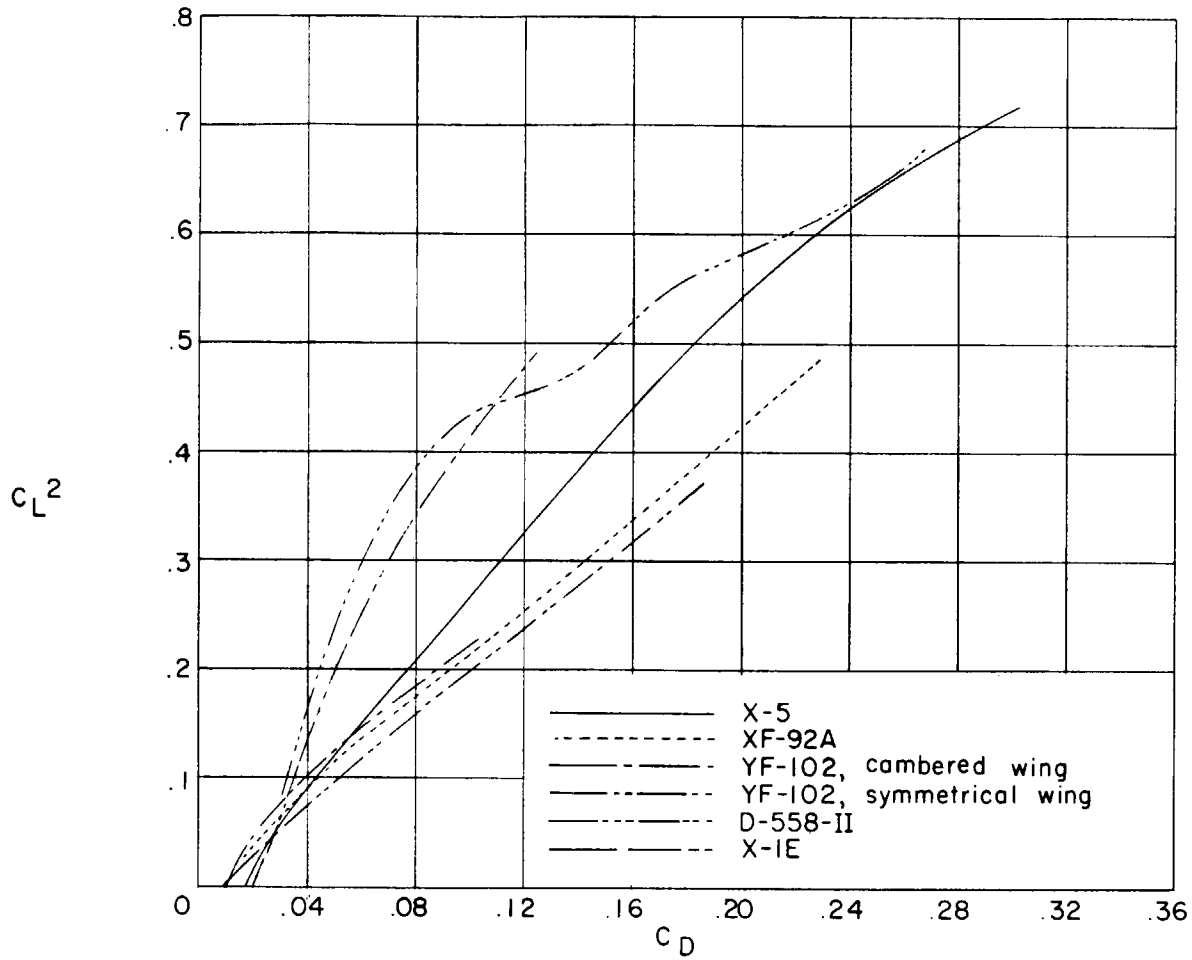

(a) M = 0.76 to 0.83.

Figure 10.- Variation of drag coefficient with lift coefficient squared in various Mach number regions.

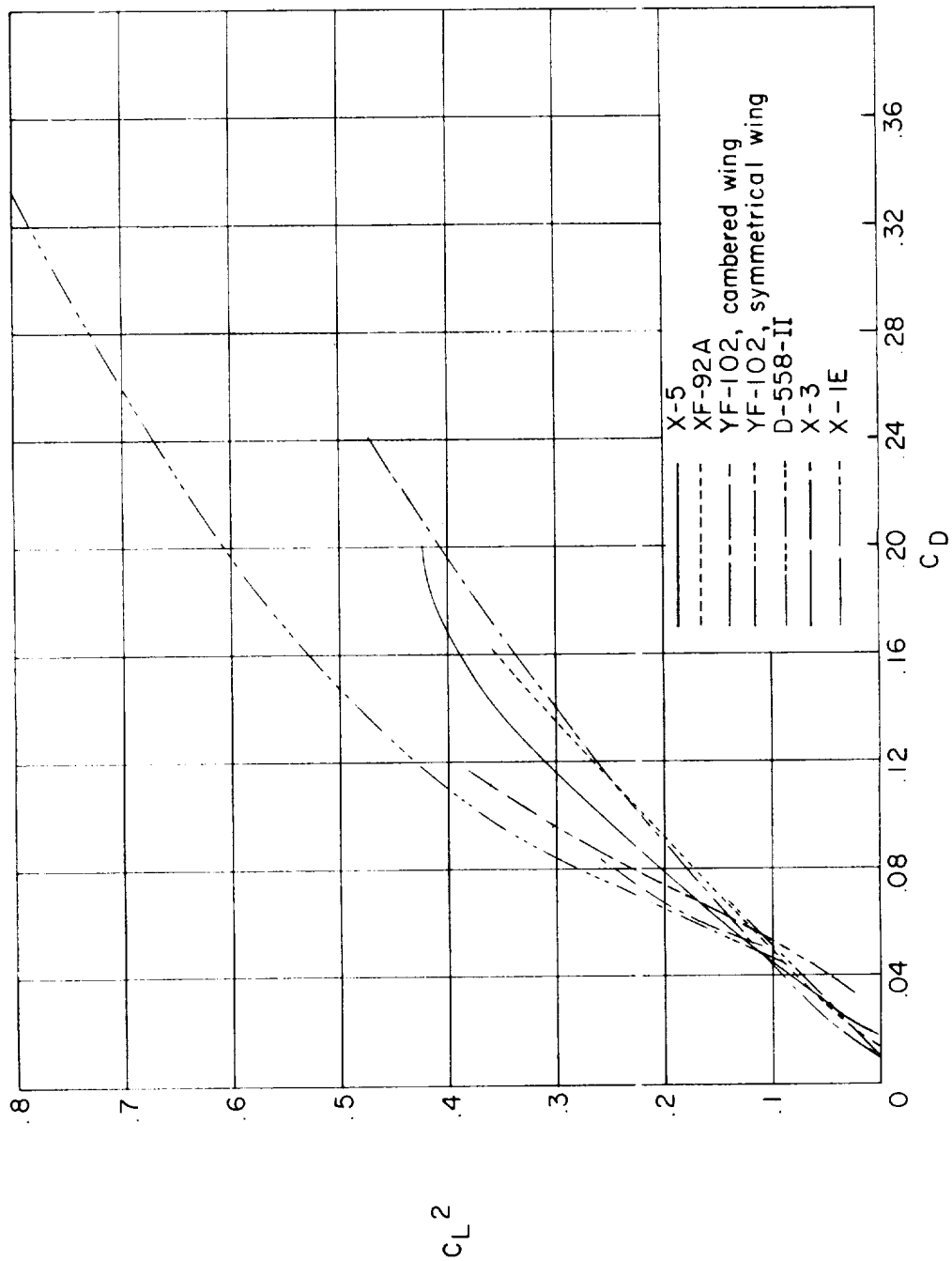

(b) M = 0.90 to 0.92.

Figure 10.- Continued.

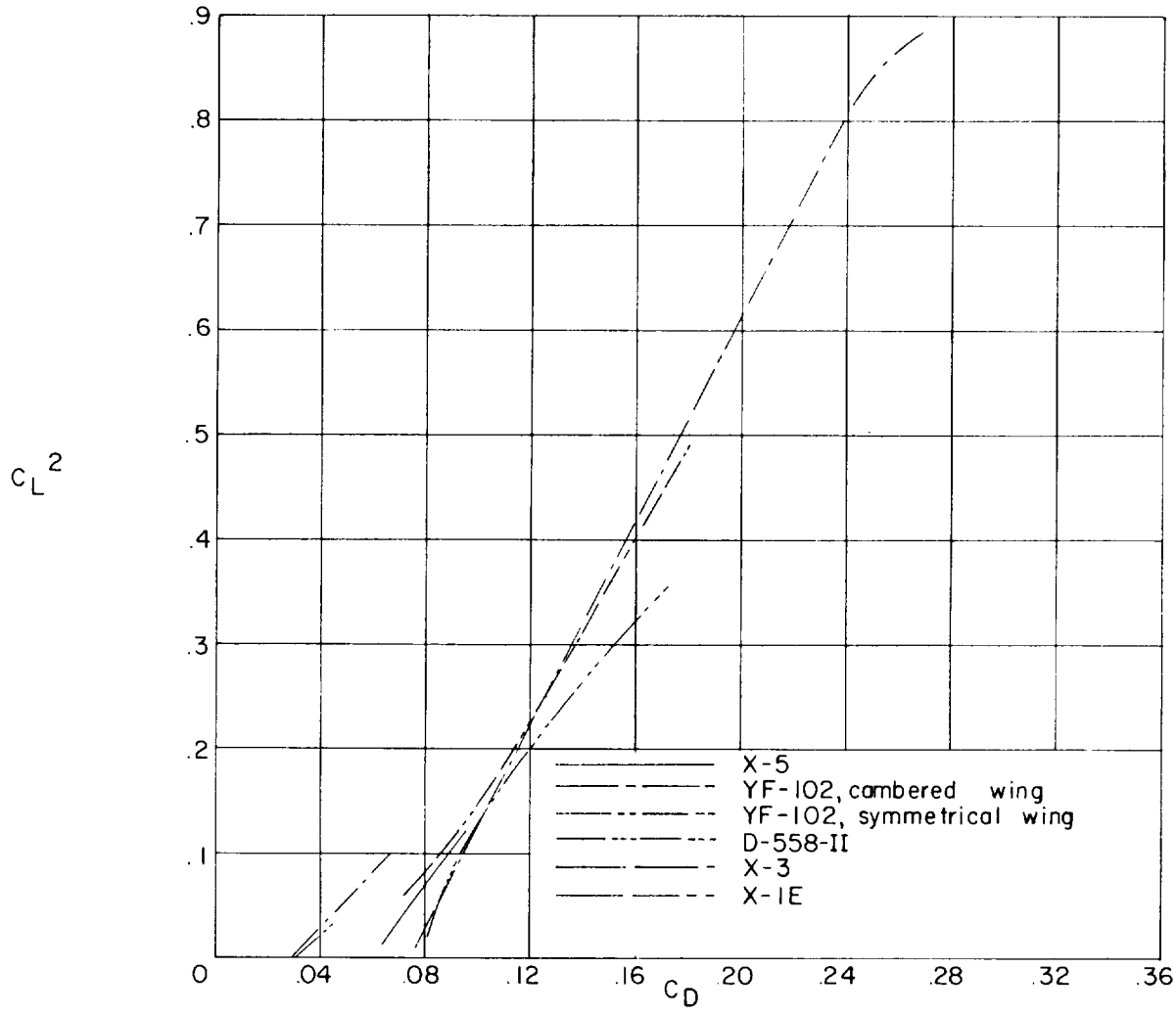

(c) M = 1.01 to 1.07.

Figure 10.- Concluded.

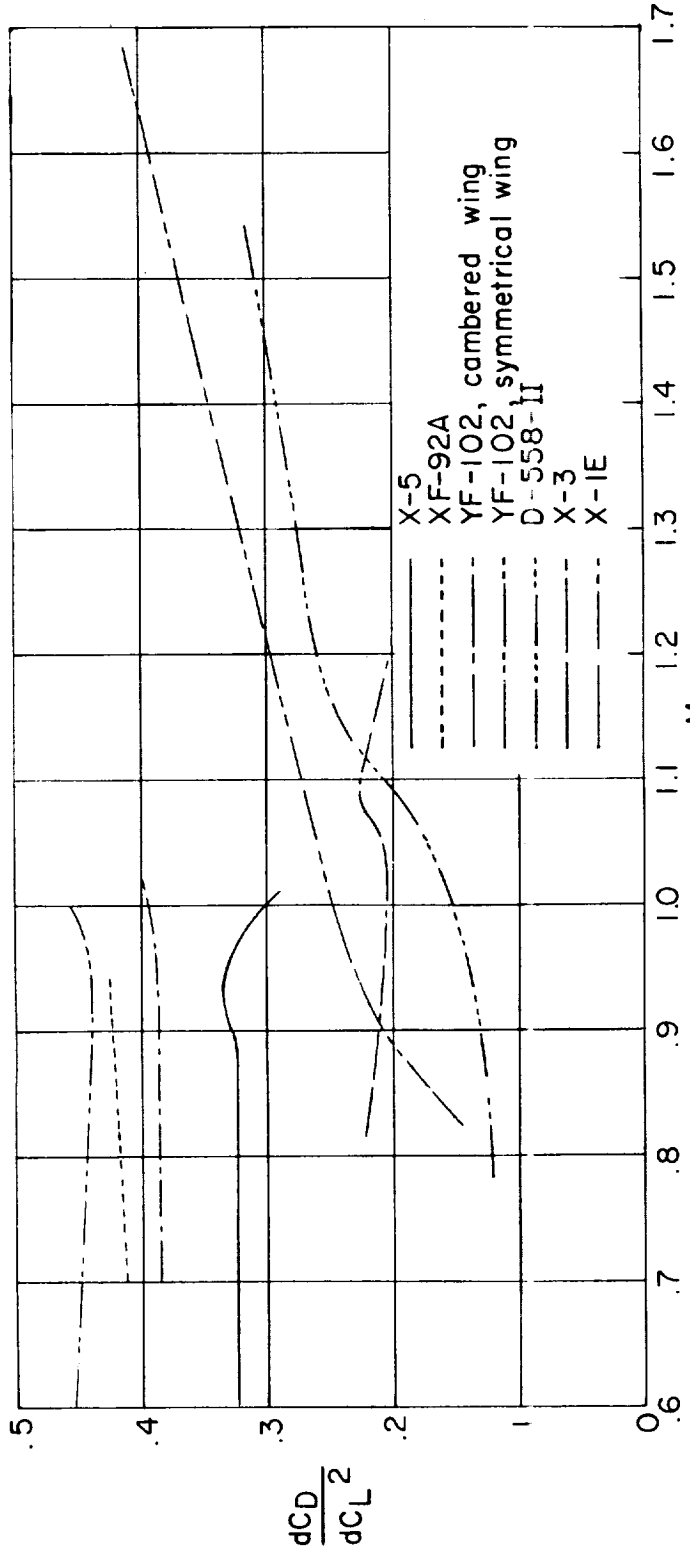

Figure 11.- Variation of drag-due-to-lift factor with Mach number. $C_L \approx 0.3$.

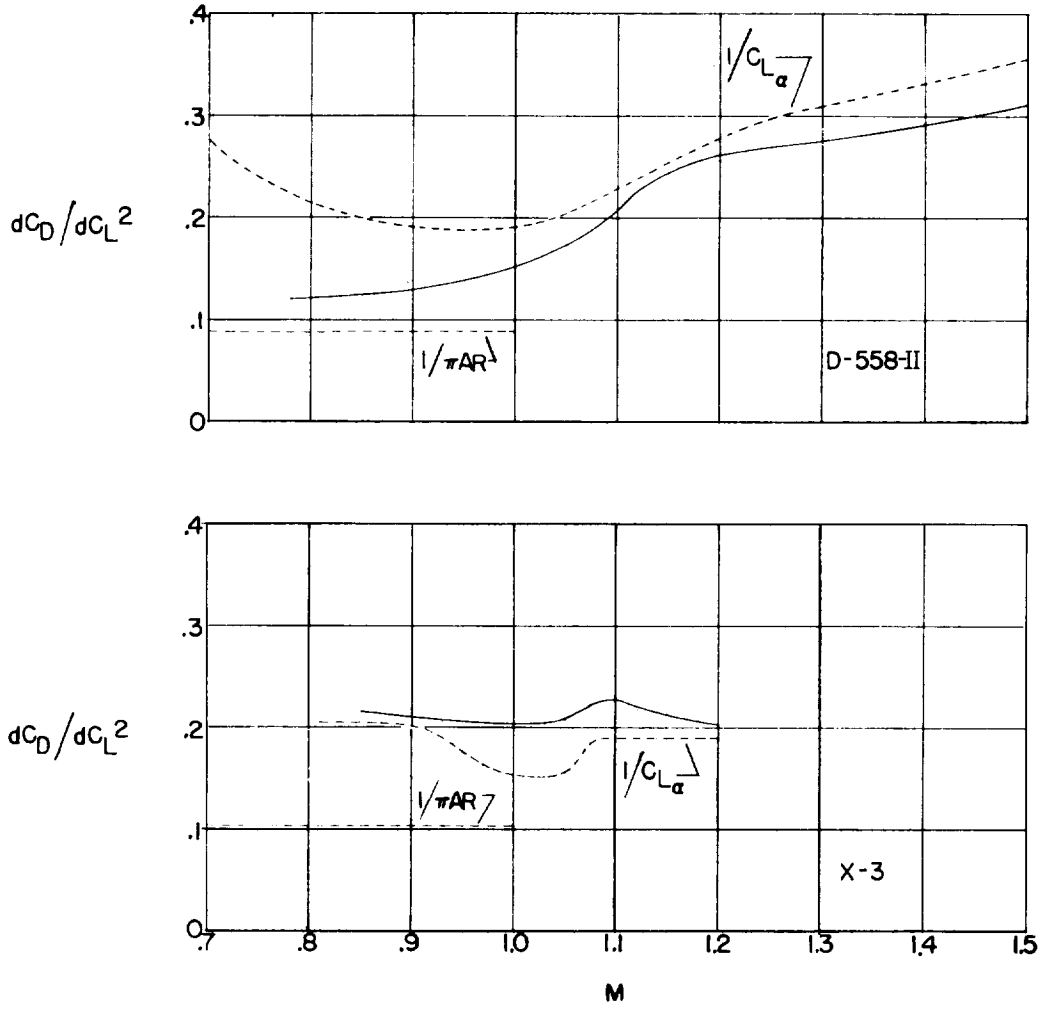

Figure 12.- Comparison of measured drag-due-to-lift factors with theoretical quantities for the D-558-II and X-3 airplanes.

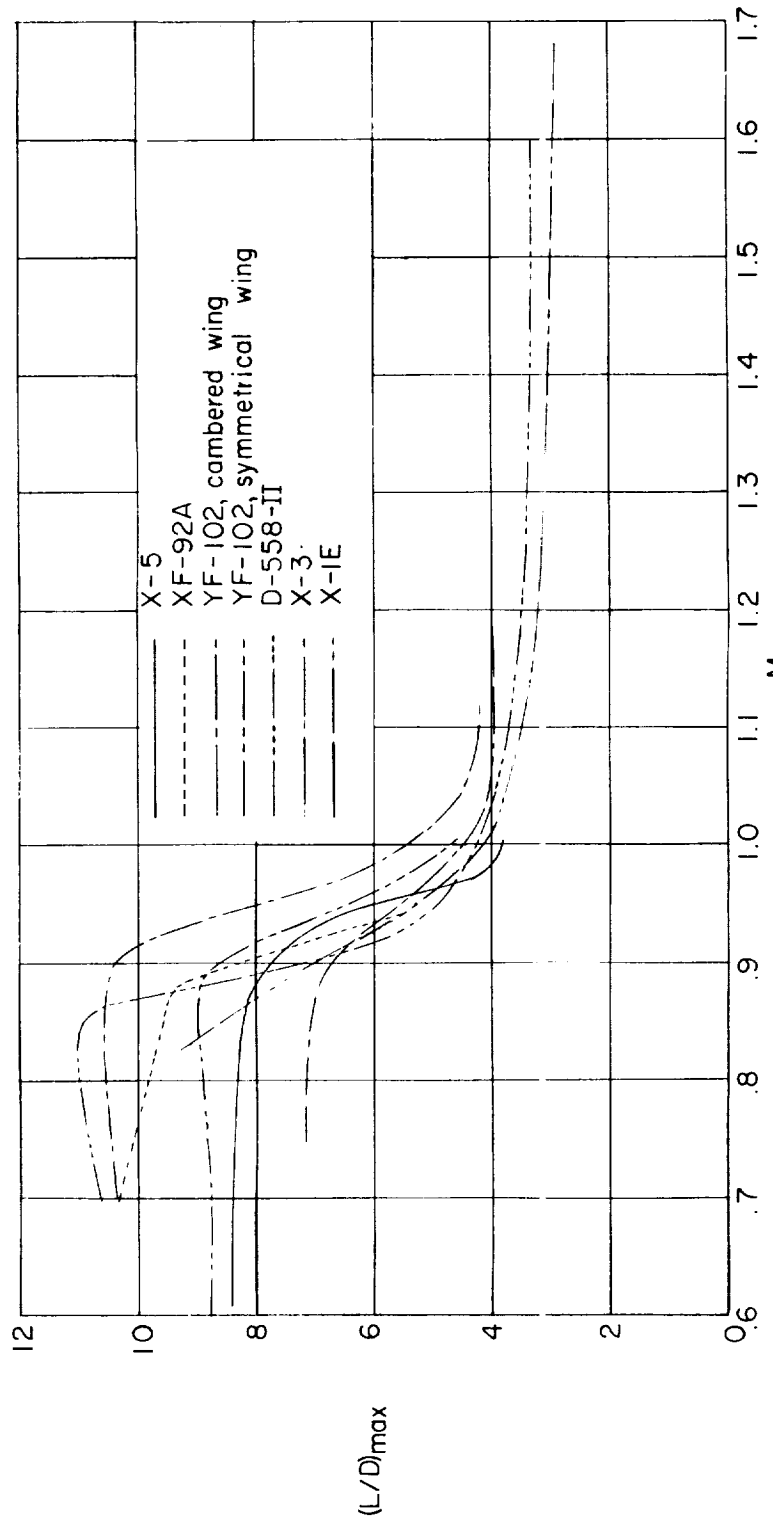

Figure 13.- Variation of maximum lift-drag ratio with Mach number.

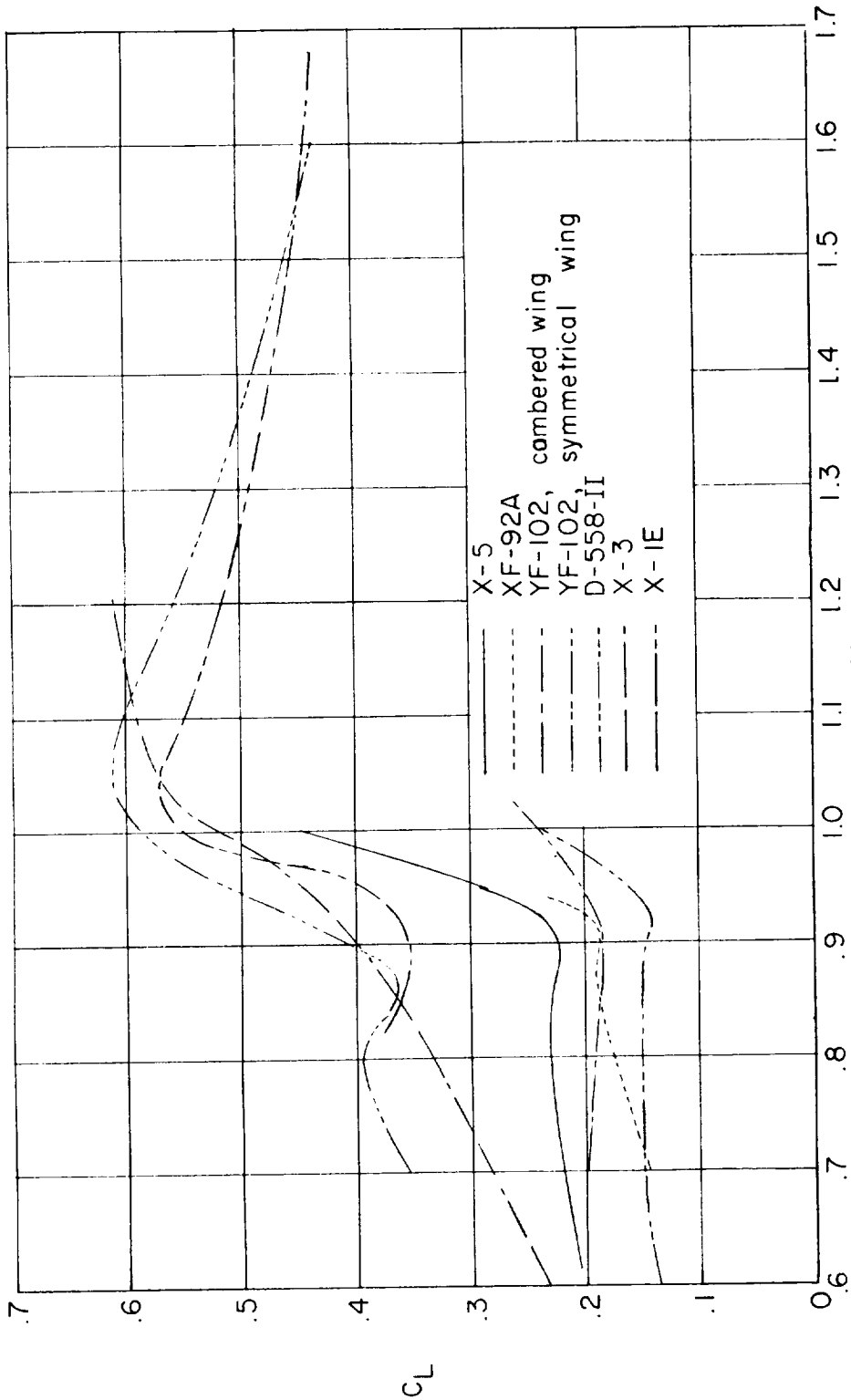

Figure 14.- Variation of lift coefficient for maximum lift-drag ratio with Mach number.

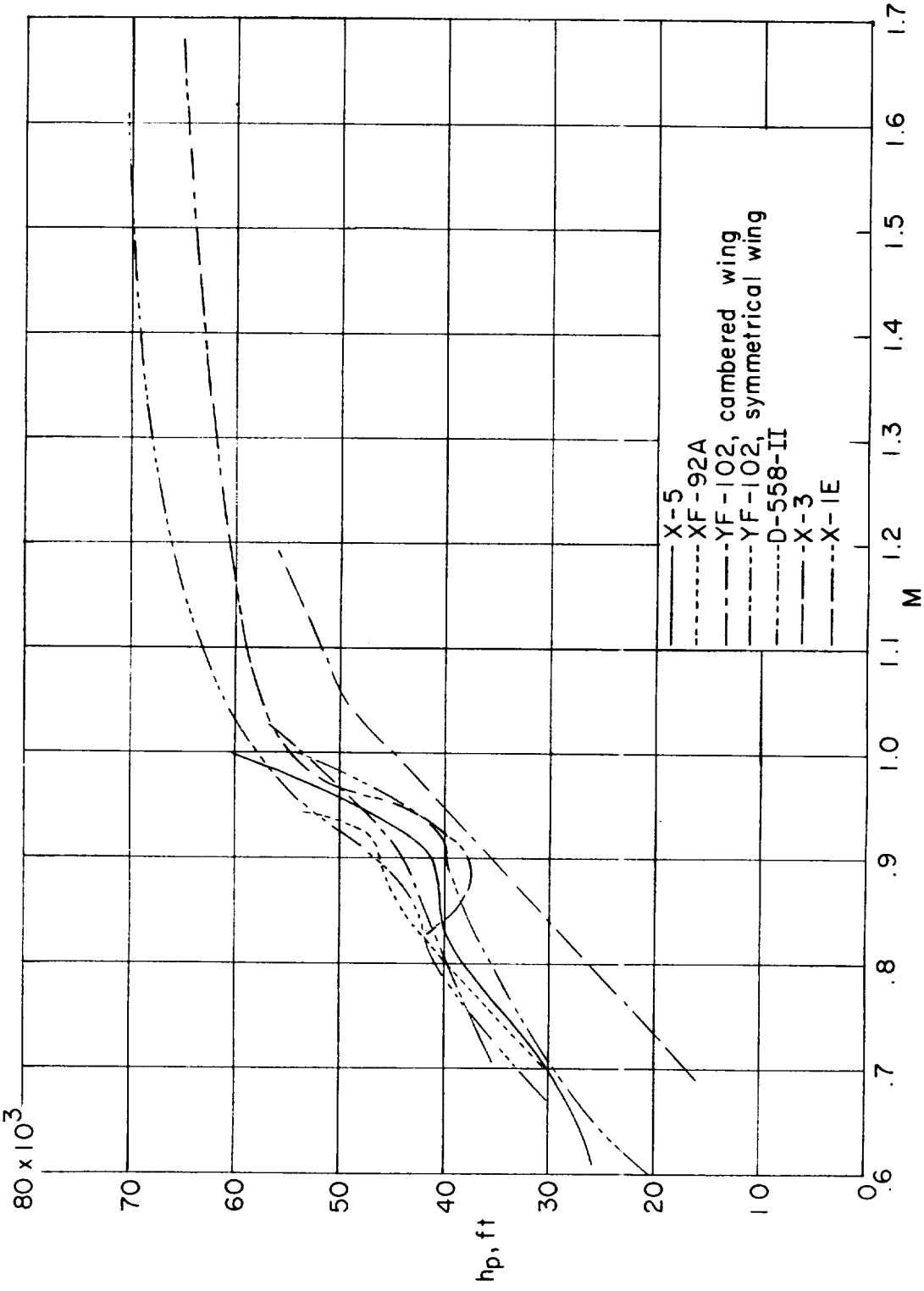

Figure 15.- Variation with Mach number of altitude for level flight at maximum lift-drag ratio.